



# Microclimate Simulation for Future Urban District under SSP/RCP: Reflecting changes in building stocks and temperature rises

Junya Yamasaki<sup>a,\*</sup>, Yasutaka Wakazuki<sup>b</sup>, Satoru Iizuka<sup>a</sup>, Takahiro Yoshida<sup>c</sup>,  
Ryoichi Nitani<sup>d</sup>, Rikutarō Manabe<sup>d</sup>, Akito Murayama<sup>d</sup>

<sup>a</sup> Graduate School of Environmental Studies, Nagoya University, Furo-cho, Chikusa, Nagoya, Aichi 464-0814, Japan

<sup>b</sup> College of Science, Ibaraki University, 2-1-1 Bunkyo, Mito, Ibaraki 310-8512, Japan

<sup>c</sup> Center for Spatial Information Science, The University of Tokyo, 5-1-5 Kashiwanoha, Kashiwa, Chiba 277-8568, Japan

<sup>d</sup> School of Engineering, The University of Tokyo, 7-3-1 Hongo, Bunkyo, Tokyo 113-8656, Japan

## ARTICLE INFO

### Keywords:

Climate change adaptation  
District scale  
Computational fluid dynamics  
General circulation model  
Urban planning

## ABSTRACT

Climate change adaptation is crucial to be addressed with specific considerations at smaller spatial scales, such as the district level, not only at the national or municipal levels. Computational fluid dynamics (CFD) analysis is particularly effective in evaluating local heat-related measures, with accumulated knowledge on future microclimate projections. In this context, it is desirable to project not only future weather conditions but also urban forms, aligning with the development trends for each scenario, and to understand the effect of each change on microclimates. Therefore, this study conducted a future microclimate simulation that reflected both changes in building stocks and temperature rises based on the Shared Socioeconomic Pathways (SSP) and Representative Concentration Pathways (RCP), focusing on an urban central district in Japan. The changes in building stocks by SSP were determined through expert judgment by researchers, including members engaged in urban planning in the district. The temperature rises by SSP/RCP were determined by referencing a statistically downscaled climate scenario dataset from the General Circulation Model (GCM). While the results showed that air temperature (AT) increased by up to 2.7 °C due to inflow temperature rises, mean radiant temperature (MRT) decreased by up to 7.5 °C due to changes in building stocks by the 2090s above the road at 14:00 on a representative summer day. It was suggested that while future temperature rises directly affected the district-scale AT, changes in building stocks had the potential to mitigate their effects on human comfort and heat-related risk. These findings emphasize the importance of aligning these future changes based on the same scenario framework in microclimate simulations and contribute novel insights to the development of this approach.

**Abbreviations:** Air temperature, AT; Computational Fluid Dynamics, CFD; Coupled Model Intercomparison Project Phase 6, CMIP6; General Circulation Model, GCM; Large-Eddy Simulation, LES; Mean Absolute Error, MAE; Mean Radiant Temperature, MRT; Ministry of the Environment, Japan, MOE; Representative Concentration Pathways, RCP; Reynolds-Averaged Navier-Stokes, RANS; Root Mean Square Error, RMSE; Shared Socioeconomic Pathways, SSP; Sixth Assessment Report, AR6; Standard New Effective Temperature, SET\*; Universal Thermal Climate Index, UTCI; Weather Research and Forecasting, WRF; Wet-Bulb Globe Temperature, WBGT.

\* Corresponding author.

E-mail address: [yamasaki.junya.i5@f.mail.nagoya-u.ac.jp](mailto:yamasaki.junya.i5@f.mail.nagoya-u.ac.jp) (J. Yamasaki).

<https://doi.org/10.1016/j.uclim.2024.102068>

Received 29 January 2024; Received in revised form 30 June 2024; Accepted 16 July 2024

Available online 17 August 2024

2212-0955/© 2024 The Author(s). Published by Elsevier B.V. This is an open access article under the CC BY license (<http://creativecommons.org/licenses/by/4.0/>).

## 1. Introduction

According to the IPCC Sixth Assessment Report (AR6), human influence has warmed the global climate at an unprecedented rate in at least the last 2000 years (IPCC, 2021). The best estimate of human-caused global surface average temperature rise from 1850 to 1900 to 2010–2019 is 1.07 °C, and future temperature rise by the end of the 21st century is projected to be 1.0–1.8 °C under SSP1-1.9, 2.1–3.5 °C under SSP2-4.5, and 3.3–5.7 °C under SSP5-8.5 (the scenario framework is described below) (IPCC, 2021). Climate change is already affecting many weather and climate extremes in every region across the world, and changes in extremes, including heat events, are projected to increase in frequency and intensity (IPCC, 2021). Particularly in urban areas, human-caused warming is intensifying locally due to the heat island phenomenon in addition to climate change. Combining climate change conditions with urban growth scenarios, future urbanization in many countries will amplify the projected temperature warming and the frequency of heat events (Grossman-Clarke et al., 2017; Kaplan et al., 2017; Li et al., 2018; Doblas-Reyes et al., 2021).

These trends are also evident in Japan. According to the Ministry of the Environment, Japan (MOE), the average temperature rise in Japan from 1898 to 2019 is 1.24 °C, exceeding the global temperature rise over the same period (MOE, 2020). The future temperature rise in Japan by the end of the 21st century is projected to be 1.4 °C under RCP2.6 and 4.5 °C under RCP8.5 (MOE, 2020). The annual number of days with maximum temperatures exceeding 35 °C, an index often used in Japan, has significantly increased nationwide from the past to the present, and is projected to continue increasing in the future (MOE, 2020). In addition, temperature rise due to the effects of urban growth has been observed nationwide. When comparing Japan's major cities such as Tokyo, Nagoya, and Osaka, with smaller cities, the average temperature rise from 1927 to 2019 was approximately 0.4–1.7 °C higher in major cities (MOE, 2020).

In response to these circumstances, there is a need to protect and promote human health against the risks posed by heat. Heat Health Action Plans including early warning and response systems are effective adaptation options for extreme heat events (IPCC, 2022). In Japan, seven specific sections framing the policies for climate change adaptation were outlined in the national climate change adaptation plan approved by the Cabinet in 2021, and basic measures regarding heat were proposed in the sections of “Human Health” and “Life of Citizenry and Urban Life” (MOE, 2021). For example, the MOE and other authorities implemented heatstroke warning alerts nationwide in April 2021 to encourage increased awareness among people regarding the rise in heat risk. Similar initiatives have been implemented at the local government level. As of February 2024, all 47 prefectures and 235 municipalities adopted local climate change adaptation plans, many of which include measures related to heat risks (A-PLAT, 2024).

While climate change adaptation at the national and municipal levels has the potential to promote system transformation, it is crucial to address them with specific considerations at smaller spatial scales, such as the district level (Luederitz et al., 2013; McNamara and Buggy, 2017; Piggott-McKellar et al., 2019; Heywood, 2023). Local communities have the potential to encourage social engagement for groups vulnerable to climate change and provide them with access to the resources they need to adapt (Shi et al., 2016; Owen, 2020; IPCC, 2022). For example, Just Communities, an initiative established in 2021, promotes the development of racially equitable and climate-resilient built environments by creating a certification system for district-scale development processes (Just Communities, 2024). District-scale sustainability rating systems such as LEED for Cities and Communities, BREEAM Communities, and the Living Community Challenge also support activities related to climate action (BREEAM, 2024; International Living Future Institute, 2024; U.S. Green Building Council, 2024). In Japan, area-based management organizations and platforms have been established to enhance the values of particular districts and are deemed promising contributors (Yasui and Izumiya, 2021; Area Management Network, 2024). When such arrangements consider social issues, including heat-related measures, the scope of their actions must adopt a long-term perspective that incorporates the potential impacts of climate change.

To develop a spatial plan for a district oriented toward climate change adaptation, it is necessary to establish scenarios that project the future environment of the target area from various perspectives. Thus, it is appropriate to reference the frameworks of Shared Socioeconomic Pathways (SSP) and Representative Concentration Pathways (RCP), which are primarily utilized in climate change research (van Vuuren et al., 2011; O'Neill et al., 2014). The SSP is a set of scenarios that project changes in global social and economic situations due to climate change impacts and related policies until 2100. The RCP is a set of scenarios that projects the concentration of greenhouse gases in the atmosphere and the resulting radiative forcing (units: W/m<sup>2</sup>) until 2100. Using these frameworks, it is possible to create general practical knowledge to construct future scenarios for urban development.

When considering urban heat-related measures, it is important to project future thermal environments in the target area. In cases where the target area is as small as a district of a few hundred square meters, which is the spatial scale of this study, computational fluid dynamics (CFD) analysis is an effective technology for projecting future urban microclimates. In recent years, studies on CFD analysis for urban microclimates have continued to advance, and their progress and challenges have been identified (Blocken, 2015; Toparlar et al., 2017; Mirzaei, 2021). Toparlar et al. (2015) referred to the application of this technology in climate change adaptation studies through their practices, and Ye et al. (2021) argued for its potential in quantifying climate change risks in cities. Zou et al. (2023) described an option for utilizing this technology for urban overheating impact assessments owing to climate change and urbanization. These CFD analyses enable the simulation of a three-dimensional microclimate that reflects the distribution of individual buildings. Such technology may contribute to decision-making regarding long-term changes in building stocks and public spaces.

Recent studies have presented various downscaling methods for broad-scale climate models, such as global circulation models (GCM), to project future microclimates at the district scale. Zou et al. (2023) described the studies by Conry et al. (2015) and Tumini and Rubio-Bellido (2016) as examples of applying CFD analysis. Conry et al. (2015) conducted dynamical downscaling of a global-scale Community Atmosphere Model and simulated microclimates for a university campus and a residential area in Chicago, USA, for future years until 2080. Tumini and Rubio-Bellido (2016) conducted statistical downscaling of the GCM and simulated microclimates for a plaza and surrounding buildings in Concepción, Chile, for 2020, 2050, and 2080. Other similar studies have used CFD analysis. Dütemeyer et al. (2013) proposed a method for identifying areas in Gelsenkirchen, Germany, requiring adaptation or

protection. Middel et al. (2015) assessed the cooling effect of trees and cool roofs in a residential neighborhood under future climate in Phoenix, USA. Emmanuel and Loconsole (2015) assessed the effectiveness of green infrastructure options under future climate in the Glasgow Clyde Valley Region, UK. Yi and Peng (2014) and Peng and Elwan (2014) proposed an outdoor-indoor coupled simulation framework to understand microclimates under climate change conditions. Fahmy et al. (2020), Tsoka et al. (2021), and Wai et al. (2021) used a CFD analysis to estimate the future building energy consumption under climate change.

The knowledge from these examples may be expected to shape long-term urban transformation toward climate change adaptation through district planning. However, to apply simulation technology to planning practices, we believe that it is desirable to project not only weather conditions, but also urban forms based on future development trends; this will facilitate comprehensive verification of how these changes might affect the future microclimate. While various methods have been proposed for inputting future weather conditions into CFD models, there are no examples of future changes in the building stocks over several decades. For example, Conry et al. (2015), Middel et al. (2015), and Emmanuel and Loconsole (2015) set cases in which heat-related measures, such as changes in land cover and roof materials, were introduced in the target areas. However, the building stocks remained essentially fixed from the base year. If cases are established for weather conditions based on the SSP/RCP in the CFD analysis, they may need to be established for changes in building stocks within the same scenario framework. To address this challenge, we believe that cross-disciplinary collaboration between climate and urban sciences, as described by Ye et al. (2021), is necessary.

However, even in urban science, no underlying method has been established to provide a robust projection of future forms of individual buildings at the district scale. This gap exists because urban transformation is delivered through a complex system involving demographic trends, economic forces, and political, social, and environmental affairs (Bosselmann, 2008; Elmqvist et al., 2019). These factors introduce uncertainties for future projections as individual stakeholders react and make decisions according to their situations. Recent studies have been conducted to project future population, land use, and GDP worldwide based on the SSP framework (e.g., Chen et al., 2020b; Gao and O'Neill, 2020; Murakami et al., 2021; Li et al., 2022; Olén and Lehsten, 2022; Wang and Sun, 2022; Wang et al., 2022). However, their spatial resolution is approximately a 1-km grid at the finest level, and these findings do not directly contribute to projecting changes in building stocks at the district scale. While some spatial analysis studies have proposed methods to estimate variables at the district/building scale mainly using downscaling approaches (e.g., Lwin and Murayama, 2009; Greger, 2015; Qiu et al., 2022; Sadeghi et al., 2023), there are no examples of such estimations based on the SSP framework in the context of climate change.

These challenges require integration of knowledge from science and practice into scenario development (von Wirth et al., 2014; Caldarice et al., 2021). It is appropriate not to use only objective data as a basis for projections at the district scale, but to incorporate the practical knowledge possessed by stakeholders who are actively engaged in the development of the district. Many cases exist in Japan where stakeholders have developed their district visions with the assistance of urban planning experts based on their unique historical contexts and community aspirations (Yasui and Izumiya, 2021). By having such experts participate in this study, it may be possible to model future building stocks under multiple scenarios with a reasonable basis. Examples of CFD analysis based on these processes would have great significance in terms of the practical implementation of simulation technology.

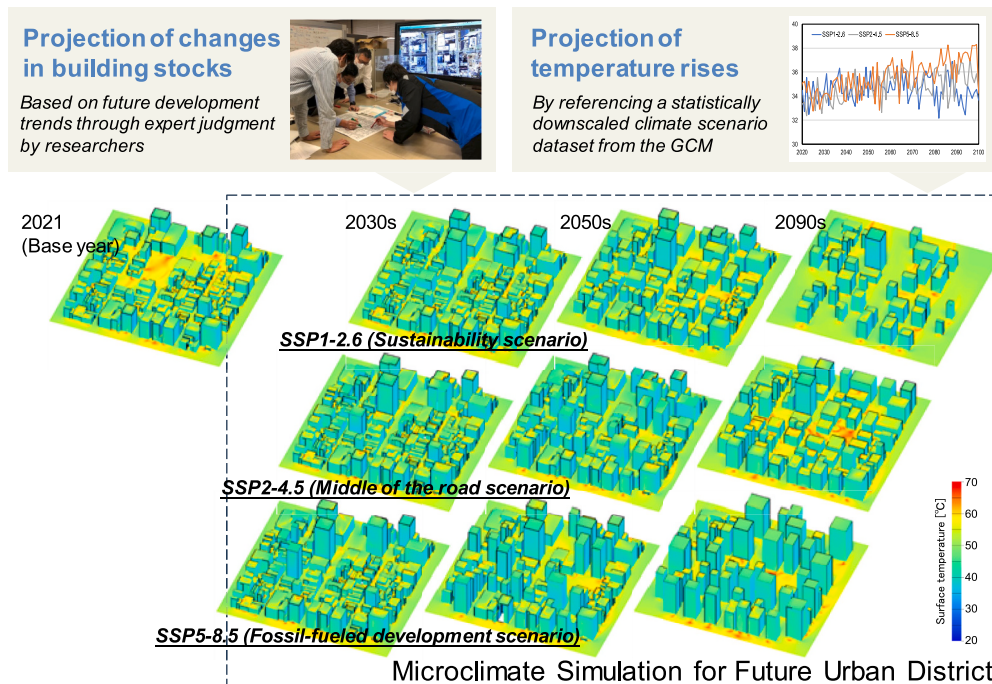


Fig. 1. Graphical summary of this study.

Therefore, this study was conducted as follows. First, we simulated the microclimate of the district-scale case study site on a representative summer day in the base year using CFD analysis, and validated its accuracy by comparing it with actual measurement results. Second, we projected changes in building stocks and temperature rises for the district on the same day in a future year based on SSP/RCP and simulated the future microclimate using the same analysis model. Changes in building stocks by SSP were determined based on future development trends through expert judgment by researchers, including members engaged in environmental improvement initiatives in the district while referencing the district master plan. Temperature rises by SSP/RCP were determined by referencing a statistically downscaled climate scenario dataset from the GCM to a 1-km grid resolution for the Japanese region.

In this study, we selected an urban center district of the Nagoya metropolitan area in Japan as a case study site, and simulated the outdoor thermal environment during summer daytime in the 2030s, 2050s, and 2090s. We focused on the thermal environment at the height of human living spaces and primarily considered the mean radiant temperature (MRT) and air temperature (AT) at 1.1 m above the ground. We verified how changes in building stocks and temperature rises in future years affect these indicators. Fig. 1 illustrates the graphical summary of this study.

These simulation results are expected to enable district stakeholders, including non-experts, to visually identify future thermal environments and share their views on climate change adaptation. Therefore, the primary aim of this study was to present new findings regarding the collaboration between climate science and urban science, rather than developing a new downscaling method for GCM to project urban microclimates with high accuracy. This exploratory research study will contribute to the further development of the planning process based on scientific evidence that can be referenced in the international urban planning realm.

## 2. Methods

This section presents the simulation method for the base year in Section 2.2, and the simulation method for future years in Section 2.3. Fig. 2 shows the method flow of this study.

### 2.1. Case study site

In this study, we selected the Nishiki 2 District, located in Nagoya City, Aichi Prefecture, Japan, as the case study site; Fig. 3 shows the location. The city is located in the middle of the mainland of Japan and functions as the regional center of the Nagoya metropolitan area, one of Japan's three major metropolitan areas. The Nishiki 2 District is located approximately 1 km from the central Nagoya Station. It has a grid-like layout and spans approximately  $400 \times 400$  m. Most buildings in the district are commercial and business facilities, with several buildings exceeding a height of 60 m. There are no parks or green spaces in these districts. In addition, an area-based management organization was established in 2018, with local stakeholders actively engaging in environmental improvement initiatives within the district (Nishiki 2 Area Management, 2024).

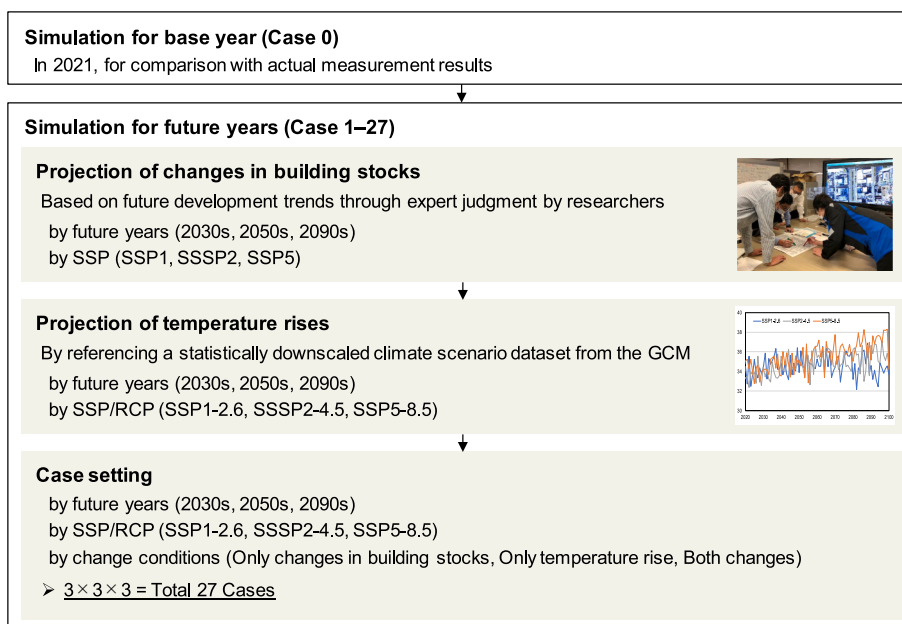


Fig. 2. Method flow of this study.

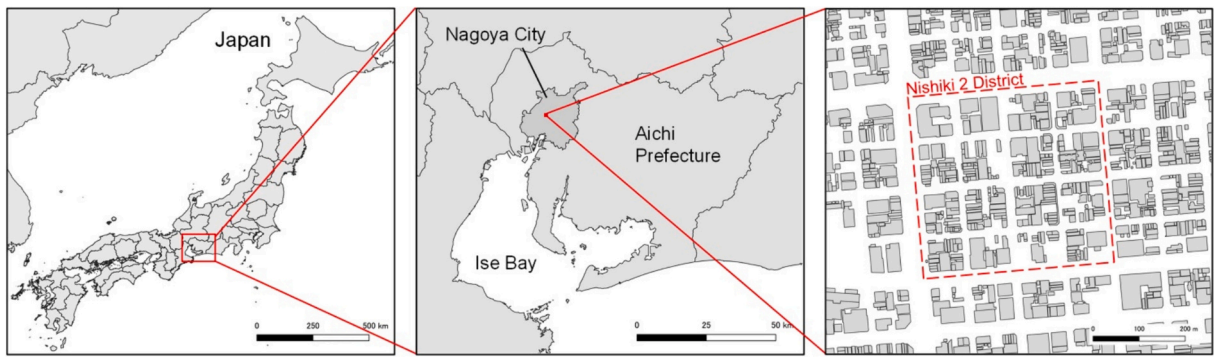


Fig. 3. Location of the Nishiki 2 District in Nagoya City, Aichi Prefecture, Japan.

## 2.2. Simulation method for the base year

This section presents the methods of the CFD analysis for a representative summer daytime in 2021, the base year (referred to as Case 0). It also presents the actual measurements conducted during the same period. The accuracy of the analysis results was tested by comparing them with the actual measurement results.

### 2.2.1. CFD analysis method

Studies on CFD analyses of urban microclimate including the coupled simulations of convection and radiation began to appear in the 1990s, and related studies have been increasing since then (e.g., Toparlar et al., 2017). In such analyses, Reynolds-Averaged Navier-Stokes (RANS) equation models are more often used than Large-Eddy Simulations (LES), primarily due to the computational costs. In RANS analyses, the standard  $k-\epsilon$  model has been frequently applied as the turbulence model, and the modified models, such as the Realizable  $k-\epsilon$  and the RNG  $k-\epsilon$  models, have often been adopted with their performances proven satisfactory in recent years (e.g., Toparlar et al., 2015; Toparlar et al., 2017; Montazeri et al., 2017; Antoniou et al., 2019). In this study, we used a CFD software and adopted a RANS analysis with the standard  $k-\epsilon$  model for high-Reynolds number turbulence, which was previously used by Kaoru et al. (2011) to analyze urban microclimate.

Fig. 4 (left) shows a 3D model of the building stocks within the Nishiki 2 District in 2021. To construct this model, we referred to GIS data from the official building survey conducted in Nagoya City in 2016. The form of each building was determined by adding the height information to the polygons. Changes in building stocks between 2016 and 2021 were identified through field audits conducted by the authors and were reflected in the model. It is important to note that only buildings were modeled in this study; other structures such as street trees, plantings, and road signs, were not included; this is because including structures other than buildings can make it more difficult to project the future urban forms.

Fig. 4 (right) shows the CFD model, and Table 1 shows overview of the CFD analysis conditions. This analysis (Case 0) targeted 10:00 to 18:00 on August 5, 2021, as a representative period during summer daytime. Although the effects of global warming are generally more evident at night, this study selected this period to discuss the most deteriorating outdoor thermal environment during the day. The analysis domain was a cubic space sufficiently surrounding the district. We referred to the data from the nearest weather observatory to determine the weather conditions for the day. Fig. 5 shows the 10-min air temperature (AT) and sunshine duration during the day. The prevailing wind direction was south, and the average wind speed was 2.8 m/s at a height of 17.8 m. There was no precipitation, and it was confirmed that the weather conditions in this area were generally representative of those in August. The time-varying weather conditions reflected in this analysis were the inflow temperature and solar radiation. We referred to the data in Fig. 5 at the corresponding time for the inflow temperature and calculated the theoretical value of the solar radiation based on the solar

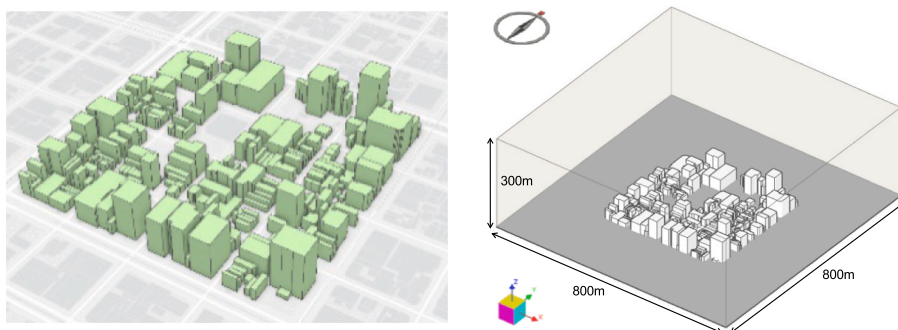
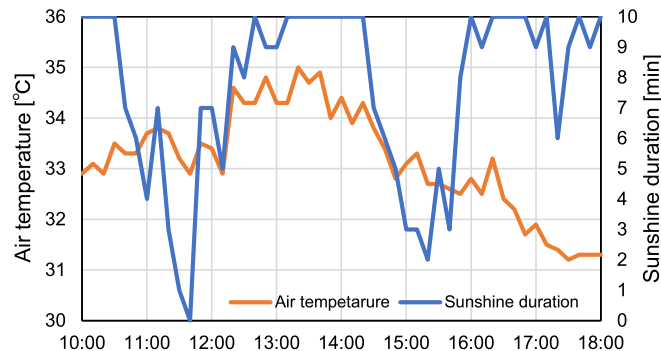


Fig. 4. Building stocks in 2021 (left) and CFD model (right) of the Nishiki 2 District.

**Table 1**  
Overview of the CFD analysis conditions.

Analysis code	FlowDesigner2022
Turbulence model	Standard k- $\epsilon$ model for the high-Reynolds number turbulence
Domain dimensions	800 m(X) $\times$ 800 m(Y) $\times$ 300 m(Z)
Mesh resolution	2,504,160 cells (structured mesh) $X_{\min} = 2.0$ m, $Y_{\min} = 2.0$ m, $Z_{\min} = 0.5$ m
Analysis period	10:00 to 18:00 on August 5, 2021 (Preliminary: 4:00 on August 3 to 10:00 on August 5)
Time step	5 min
Inflow conditions	Wind speed: 1.0 m/s, Reference height: 10 m Wind direction relative to the north: $-180^\circ$



**Fig. 5.** 10-min data from the nearest weather observatory.

azimuth at the location, assuming only direct solar radiation. Although the data in Fig. 5 indicate that the cloud cover on the day was not constant, we assumed that the cloud cover consistently reduced the direct solar radiation by 20% in this analysis. Regarding the wind direction and wind speed, we fixed the inflow condition to the southern face of the model at 1.0 m/s, referenced at a height of 10 m. This value was based on the minimum observed data during the target period in order to simulate conditions unfavorable to human comfort and heat-related risk.

We used two types of boundary conditions for the structures: the ground (asphalt) and the building surface (limestone concrete). In the thermal calculations of the ground and building surfaces, we assumed the presence of a pseudo-thickness between the inner and outer portions of the analysis domain. The heat balance on the inside surface was calculated to ensure that the sum of the solar radiation, long-wave radiation, convective heat transfer, and heat conduction into the structure was equal to 0. The heat conduction in the structure was calculated by setting the surface temperature outside the structure, the pseudo-thickness of the structure, and the thermal properties. Table 2 shows the boundary conditions of the ground and building surfaces used in this analysis. As there are no parks or green spaces, and most of the buildings are non-wooden in the district, only two types of boundary conditions were used for the structures. The ground boundary conditions were set uniformly on the entire bottom surface of the analysis domain, including the surrounding area of the district.

The MRT in the analysis results was calculated based on the radiation flux in six directions of the respective mesh. This radiation flux was calculated as the sum of the direct solar radiation and long-wave radiation from the surrounding structures based on the area-weighted average of each mesh surface (Eq. 1).

**Table 2**  
Boundary conditions for the ground and building surfaces.

Thermal properties	Ground (asphalt)	Building surface (limestone concrete)
Density [kg/m <sup>3</sup> ]	2120	2400
Specific heat [J/KgK]	921	900
Conductivity [W/mK]	0.74	1.2
Albedo	0.15	0.35
Emissivity	0.90	0.90
Pseudo-thickness [m]	0.1	0.3
Surface temperature outside the structure [°C]	24	28

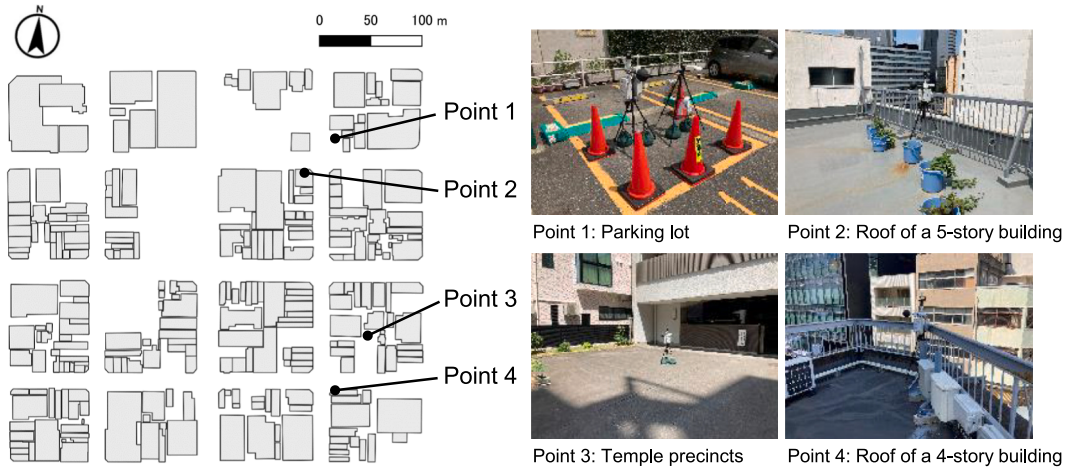


Fig. 6. Locations of the actual measurement points.

$$MRT = \frac{\sum_{i=1}^6 S_i (q_i \sigma^{-1})^{\frac{1}{4}}}{\sum_{i=1}^6 S_i} \quad (1)$$

where  $MRT$  is mean radiant temperature [K],  $S_{i,j}$  is the area of each mesh surface [ $\text{m}^2$ ],  $q_i$  is radiation flux [ $\text{W}/\text{m}^2$ ], and  $\sigma$  is Stefan Boltzmann constant [ $\text{W}/\text{m}^2\text{K}^4$ ].

### 2.2.2. Actual measurement method

We conducted actual measurements at four points in the district on August 4 and 5, 2021, from 10:00 to 18:00. The measured variables included air temperature (AT), black-bulb temperature, and wind speed, all recorded at 1-s intervals. Fig. 6 shows the locations of the measurement points, which were positioned 1.1 m above the ground or the roofs of buildings, representing locations on both the upwind and downwind sides within the district. However, these points were limited to the district's west side due to actual measurement constraints. The  $MRT$  values in the measurement results were calculated based on ISO7726 Annex B (ISO, 1998) (Eq. 2).

$$MRT = \left\{ (T_g + 273)^4 + 2.5 \times 10^8 \times V^{0.6} (T_g - T_a) \right\}^{0.25} - 273 \quad (2)$$

where  $MRT$  is mean radiant temperature [ $^{\circ}\text{C}$ ],  $T_a$  is air temperature (AT) [ $^{\circ}\text{C}$ ],  $T_g$  is black-bulb temperature [ $^{\circ}\text{C}$ ], and  $V$  is wind speed [ $\text{m}/\text{s}$ ].

### 2.3. Simulation method for future years

This section presents the methods of the CFD analysis for summer daytime in the 2030s, 2050s, and the 2090s (Case 1–27), using the same analysis model as in Section 2.2. Future years were selected based on the 20-year time periods defined in IPCC AR6: Near-term (2021–2040), Mid-term (2041–2060), and Long-term (2081–2100) (IPCC, 2021).

#### 2.3.1. Outlines

In this study, we projected future changes in building stocks and temperature rises based on SSP/RCP. There are five scenarios for SSP ranging from SSP1 to SSP5 and multiple scenarios for RCP ranging from RCP1.9 to RCP8.5, necessitating the selection of an appropriate combination. O'Neill et al. (2014) identified four priority scenario combinations (Tier 1): SSP1-2.6, SSP2-4.5, SSP3-7.0, and SSP5-8.5—for example, SSP1-2.6 indicates a combination of SSP1 and RCP2.6. The findings summarized in IPCC AR6 are primarily based on these scenarios. Referring to them, we selected three representative scenarios: SSP1-2.6 as the Sustainability scenario, SSP2-4.5 as the Middle of the road scenario, and SSP5-8.5 as the Fossil-fueled development scenario.

Table 3 shows the simulation case setting for future years. Based on Case 0 in Section 2.2, we set cases that reflected only changes in building stocks by SSP/RCP (Case 1–9), cases that reflected only temperature rise by SSP/RCP (Case 10–18), and cases that reflected both changes by SSP/RCP (Case 19–27). These case setting facilitated the comparison of the effects of changes in building stocks and temperature rises on the district's microclimate.

**Table 3**

Case setting of CFD analysis for future years.

Scenario		2021	2030s	2050s	2090s
Only changes in building stocks	SSP1-2.6	Case 0	Case 1	Case 2	Case 3
	SSP2-4.5	“	Case 4	Case 5	Case 6
	SSP5-8.5	“	Case 7	Case 8	Case 9
Only temperature rise	SSP1-2.6	“	Case 10	Case 11	Case 12
	SSP2-4.5	“	Case 13	Case 14	Case 15
	SSP5-8.5	“	Case 16	Case 17	Case 18
Both changes	SSP1-2.6	“	Case 19	Case 20	Case 21
	SSP2-4.5	“	Case 22	Case 23	Case 24
	SSP5-8.5	“	Case 25	Case 26	Case 27

### 2.3.2. Projection of changes in building stocks

Chen et al. (2020a) developed a Japanese version of the SSP that reflects the social and economic situation in Japan, and nationwide future population estimation data for each municipality based on the Japanese version of the SSP was published (A-PLAT, 2021). In addition, Nagoya City formulated a city master plan summarizing the future vision of the urban structure until 2030 (Nagoya City, 2020). The area-based management organization in the Nishiki 2 District developed a district master plan summarizing the district's future vision until 2030, with the assistance of urban planning experts (Nishiki 2 District Community Development Council, 2011). Referring to them, we projected changes in building stocks based on future development trends in the Nishiki 2 District until the 2090s under SSP1, SSP2, and SSP5. Given the participation of four authors, some of whom are researchers engaged in urban development in the district, we refer to this process as expert judgment. Table 4 shows the expert judgment results.

First, we determined the future urban structure of Nagoya City, vision statements, development trends, and new building scopes in the Nishiki 2 District based on each scenario. These were referenced to the Japanese version of the SSP (Chen et al., 2020a), particularly for SSP1; the city master plan and the district master plan were referenced (Nagoya City, 2020; Nishiki 2 District Community Development Council, 2011). Second, we assessed the rationality of land use in the district to identify redevelopment sites and buildings in each target year. This assessment considered factors such as the age of existing buildings, the desirability of preservation for historical buildings, and the form and size of each building site with reference to the district master plan (Nishiki 2 District Community Development Council, 2011). Third, on a site-specific and scenario basis, we decided whether the building reconstruction approach should be collective with site consolidation or individual. These decisions considered future development pressures with reference to Nagoya City's population estimates (A-PLAT, 2021). However, the total floor area of the buildings was not necessarily proportional to the population estimates because the district was located in a particularly central urban area.

### 2.3.3. Projection of temperature rises

This study determined future weather conditions by referencing the idea of pseudo global warming method proposed by Kimura and Kitoh (2007). The fundamental concept of this method involves incorporating the difference between current and future physical quantities of climate projection data into current weather conditions. We focused solely on the temperature rise as the impact of climate change on weather conditions, adjusting only the inflow temperature of Case 0 to reflect the temperature rise from 2021. In the field of meteorology, the Coupled Model Intercomparison Project Phase 6 (CMIP6) was implemented to improve the accuracy of future climate projection data. Subsequently, Ishizaki et al. (2022) conducted a statistical downscaling of GCMs based on CMIP6 and constructed a bias-corrected climate scenario dataset at a 1-km grid resolution over Japan. We referred to the physical quantities of the average maximum temperature in August for MRI-ESM2-0, a GCM in this dataset, to determine the temperature rise from 2021.

The projection process of the temperature rise by SSP/RCP is shown below. Fig. 7 shows the future projections of the average maximum temperature in August by SSP/RCP in the grid on which the Nishiki 2 District is located. Table 5 shows their average values for 21 years at around 2021, 2030, 2050, and 2090 (10 years before and after) and their differences from the value in 2021 by SSP/RCP. We determined the inflow temperature for each SSP/RCP by uniformly adding these differences to the inflow temperature in Case 0. For example, since the inflow temperature at 12:00 on August 5, 2021, in Case 0, was 33.4 °C, the inflow temperature at 12:00 on the same day in the 2090s was determined to be 36.3 °C.

## 3. Results










This section presents the simulation results for the base year (Case 0) in Section 3.1, and the simulation results for future years (Case 1–27) in Section 3.2.

### 3.1. Simulation results for the base year

Fig. 8 shows the spatial distributions of the MRT and AT at 1.1 m above the ground for the entire district every two hours from 10:00 for Case 0. The effects of building shade were evident in the MRT results, especially due to the grid-like layout of the district. Fewer buildings obstructed direct solar radiation when the sun aligned with the roads, causing an increase in the surface temperature of the roads. Consequently, the values were higher above the north-south road at 12:00 and above the east-west road at 16:00. In addition, the values tended to be higher near building surfaces exposed to direct solar radiation. The inflow temperature directly influenced the

**Table 4**

Expert judgment results for future changes in building stocks in the Nishiki 2 District.\*

Scenario name		SSP1 (Sustainability scenario)	SSP2 (Middle of the road scenario)	SSP5 (Fossil-fueled development scenario)
Urban structure of Nagoya City		Well-established compact and networked urban structure, forming mixed-use urban areas centered around train stations.	Few major changes in urban structure from the 2020s, while slow growth with individual building reconstructions.	Highly concentrated urban structure, with business and commercial facilities cluster at its center and expanding residential suburbs.
	Vision statements	Urban area where people live and work	Urban areas under moderate growth	Urban area where people work and visit
	Development trends	Development will peak in the 2050s, after which the buildings will be properly demolished and the site will be used for multiple purposes.	Development pressure in the 2020s will continue moderately until the 2090s.	Intensive development due to deregulation will continue until the 2090s.
	New building scopes	Medium-rise buildings with a mix of residential, commercial, and business uses (FAR: 400–600%)	Med-to-high-rise buildings for commercial and business uses (FAR: 600–800%)	High-rise buildings for commercial and business uses (FAR: 800%)
Nishiki 2 District	Building stocks in the 2030s			
	Building stocks in the 2050s			
	Building stocks in the 2090s			

\* Orange buildings are constructed after the base year.

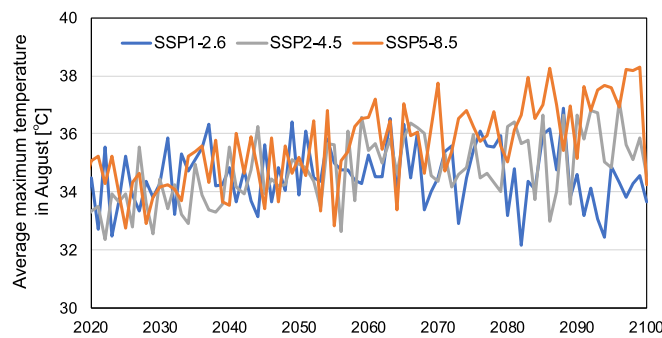


Fig. 7. Future projections of the average maximum temperature in August by SSP/RCP.

**Table 5**

Average values of average maximum temperature in August for 21 years around 2021, 2030, 2050, and 2090 and their differences from the value in 2021 by SSP/RCP.

Category		2021	2030	2050	2090
Average values for 21 years around target year [°C]	SSP1-2.6	33.9	34.4	34.7	34.3
	SSP2-4.5	33.6	34.0	34.9	35.3
	SSP5-8.5	34.0	34.4	35.1	36.9
Difference from the average value in 2021 [°C]	SSP1-2.6	–	0.6	0.8	0.4
	SSP2-4.5	–	0.4	1.3	1.7
	SSP5-8.5	–	0.4	1.1	2.9

AT results, with values for the entire district increasing at 14:00 and tending to be higher near building surfaces exposed to direct solar radiation.

We identified four points within the analysis model for actual measurements and compared diurnal changes in each indicator. Fig. 9 shows the diurnal changes in the analysis values and the measured values of the MRT and AT at 1.1 m above the ground or the roofs of the buildings at these points. Table 6 shows the mean absolute error (MAE), root mean square error (RMSE), and coefficient of determination ( $R^2$ ) between the analysis and the measured values. The MAE, RMSE, and  $R^2$  were calculated based on 49 data points, corresponding to the number of time points every 10 min from 10:00 to 18:00.

As confirmed by Fig. 9, the analysis and the measured values roughly showed similar diurnal changes. Focusing on the MRT results, for example, Point 3 was shaded from approximately 14:00, and Point 4 was exposed to direct solar radiation from approximately 12:00, with the analysis values generally reflecting these conditions. Since Points 1 and 2 were located in areas with limited shade hours, the analysis values remained high throughout the day. Each indicator in Table 6 showed relatively large errors at Points 2 and 4. These points were located above the roofs of buildings; thus, their surfaces may have been more prone to heating than those in the analysis model.

Focusing on the AT results, at Points 1, 3, and 4, the analysis and the measured values peaked between 13:00 and 14:00. At Points 2, 3, and 4, differences between the two values remained within 2.0 °C for almost the entire period. At Point 1, this difference temporarily exceeded 3.0 °C around 14:00, likely owing to shading from unmodeled structures such as signboards around the parking lot. Each indicator in Table 6 showed relatively large errors at Points 1 and 3, possibly affected by surrounding structures because these points were located above the ground.

The accuracy of this analysis model was compared with that of previous studies. Tominaga et al. (2023) reviewed the progress of studies on the accuracy of microclimate simulations, and introduced the study by Antoniou et al. (2019), which simulated an urban area in Cyprus. The analysis model of Antoniou et al. (2019) is similar to ours in that the shapes of buildings were simply modeled, and the building and ground surfaces were uniformly set using limited types of materials. In their study, the MAE for AT and surface temperature between the analysis and the measured values were 1.35 °C and 2.37 °C, respectively. Compared to them, our analysis model may have a larger error in MRT, partly due to certain assumptions made to aid analyzing future conditions. In particular, the rate of decrease in direct solar radiation and constant wind direction and speed are one of the major sources of errors. As this section is primarily aimed to reproduce a representative summer day rather than a specific day, we concluded that this was achieved in Case 0 despite some issues with the analysis accuracy.

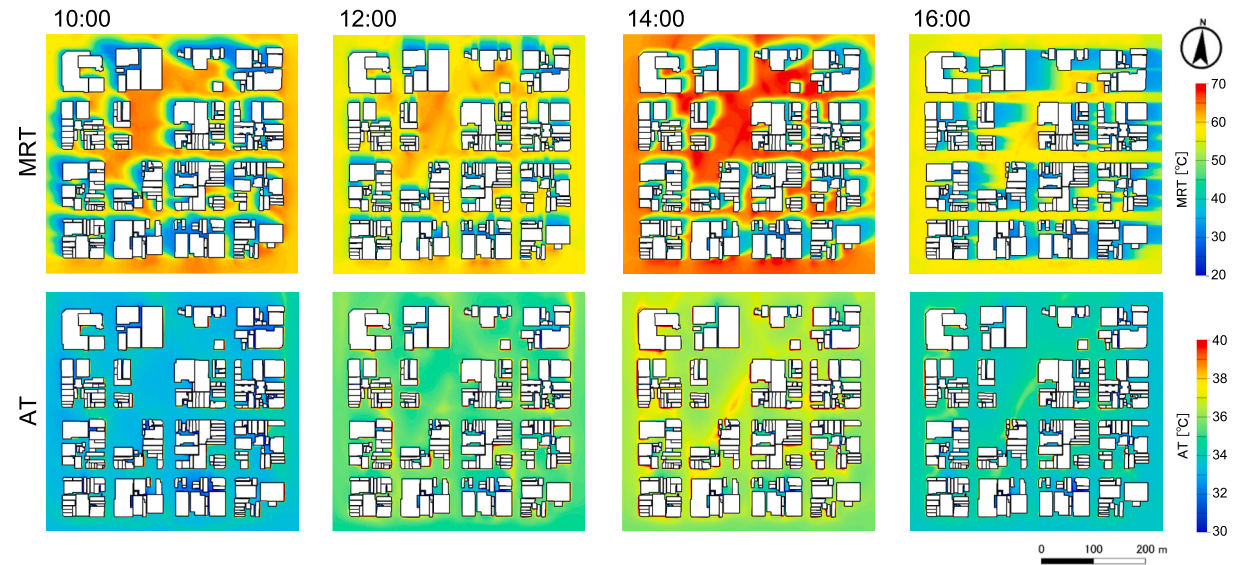


Fig. 8. Analysis results (Case 0): spatial distributions of the MRT and AT at 1.1 m above the ground.

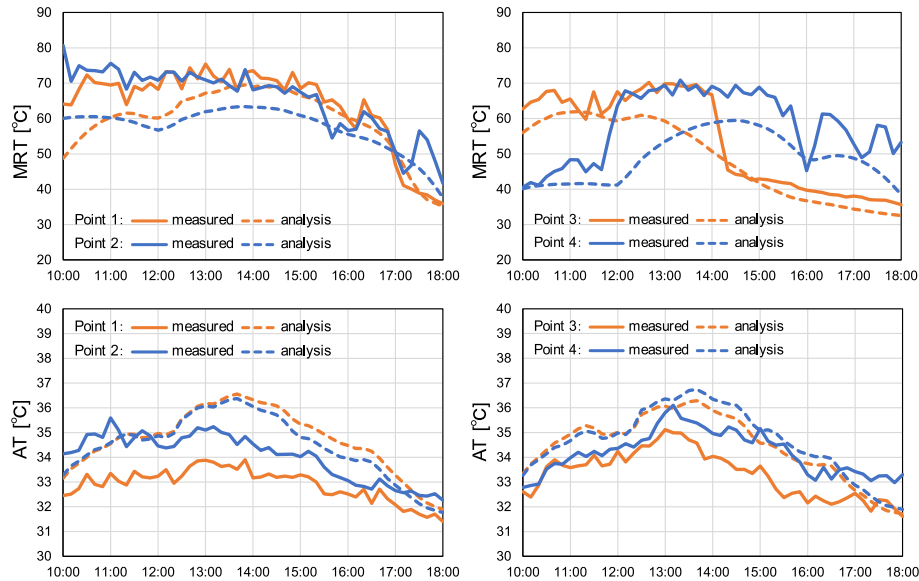


Fig. 9. Comparison of analysis results (Case 0) and the measured results: diurnal changes of the MRT and AT at 1.1 m above the ground or the roofs of the buildings.

**Table 6**  
Calculation results of the mean absolute error (MAE), root mean square error (RMSE), and coefficient of determination ( $R^2$ ) between the analysis and the measured values.

Indicator	MRT				AT			
	Point 1	Point 2	Point 3	Point 4	Point 1	Point 2	Point 3	Point 4
MAE [°C]	5.5	8.5	5.4	9.4	1.8	0.8	1.2	0.8
RMSE [°C]	6.9	9.7	6.7	11.0	2.0	0.9	1.3	0.9
$R^2$ [–]	0.8	0.7	0.9	0.6	0.8	0.6	0.8	0.8

### 3.2. Simulation results for future years

Section 3.2.1 presents the results at 14:00 from 2021 to the 2090s, as a representative time for each year. Section 3.2.2 presents the results of diurnal changes from 10:00 to 18:00 in the 2090s.

#### 3.2.1. Results at 14:00 from 2021 to the 2090s

**Fig. 10** shows the spatial distributions of the MRT and AT at 1.1 m above the ground for the entire district at 14:00 for Case 0 and 19–27. Thus, it is possible to compare the results when both changes in building stocks and temperature rises are reflected from 2021 to the 2090s under each SSP/RCP. In addition, we selected two road, each running north-south and east-west through the center of the district as the representative spaces, calculating the average MRT and AT at 1.1 m above each road. These calculations were conducted using the analysis values from all meshes corresponding to 1.1 m above the ground in each road space within the district. **Fig. 11** shows the changes in these average values at 14:00 each year for the same SSP/RCP cases. For example, under SSP1-2.6, the values at 14:00 are shown for Case 0, 1–3, 10–12, and 19–21. Thus, it is possible to compare the results reflecting only changes in building stocks, only temperature rise, and both changes from 2021 to the 2090s under each SSP/RCP. **Table 7** shows the differences in these average values between 2021 and the 2090s at 14:00 under each SSP/RCP, serving as a supplement to **Fig. 11**.

**3.2.1.1. MRT results.** Focusing on the MRT results in **Fig. 10**, the values for the entire district were largely affected by the distribution of shade owing to building stocks. Under SSP1-2.6, the area exposed to direct solar radiation, hereinafter referred to as the sunlit area, largely increased in the 2090s owing to the increase in open space (Case 19–21). Under SSP2-4.5, although there were no major changes in the total floor area of building stocks until the 2090s, the sunlit area increased owing to collective building reconstruction (Case 22–24). Under SSP5-8.5, the shaded area increased until the 2090s, owing to an increase in the number of high-rise buildings. Simultaneously, the MRT values for the sunlit area gradually increased over the decades owing to the expansion of the building sides and increases in their surface temperatures (Case 25–27).

Focusing on the MRT results for the north-south road in **Fig. 11** under any SSP/RCP, the numerical changes were larger in the cases of only changes in building stocks (blue line) than only temperature rise (red line). Under SSP1-2.6, in the cases of only temperature rise (Case 10–12), the differences from the base year were within 0.4 °C for each year. In the cases of only changes in building stocks (Case 1–3), the value decreased by 6.2 °C until the 2050s owing to an increase in the shaded area, and in the 2090s, the value exceeded the base year by 2.0 °C owing to an increase in the sunlit area. Even under SSP2-4.5 and SSP5-8.5, the numerical changes were relatively small in the cases of only temperature rise (Case 13–18), and the maximum differences were 1.0 °C under SSP2-4.5 and 2.0 °C under SSP5-8.5. In contrast, in the cases of only changes in building stocks (Case 4–9), the maximum differences from the base year were 7.0 °C under SSP2-4.5 and 7.5 °C under SSP5-8.5. In the cases of only changes in building stocks, the values in the 2090s followed the order of SSP1-2.6, SSP2-4.5, and SSP5-8.5 (Case 3, 6, and 9), indicating that they were largely affected by the shaded area. Based on these results, the numerical changes in the cases of both changes (Case 19–27, yellow line) tended to be close to those in the cases of only changes in building stocks (Case 1–9).

Focusing on the MRT results for the east-west road in **Fig. 11**, the overall trend was similar to that for the north-south road, and the numerical changes were larger in the cases of only changes in building stocks (Case 1–9, blue line) than only temperature rise (Case 10–18, red line). The values for all cases were higher than those for the north-south road mainly because of the shading angle of the buildings at 14:00. In the cases of only changes in building stocks (Case 1–9), the numerical changes from the base year tended to be smaller than those for the north-south roads, mainly because of the relatively fewer changes in building stocks along the east-west road.

**3.2.1.2. AT results.** **Fig. 10** shows that the entire district's values depended on the inflow temperature. Higher values were observed near the building surfaces exposed to direct solar radiation, where warm air diffused. In shaded areas, the values tended to be lower owing to the effect of surrounding surface temperatures. Under SSP1-2.6, there were fewer areas where warmed air accumulated because of the decrease in the number of buildings in the 2090s (Case 21). Under SSP2-4.5, there was a relatively high number of buildings even in the 2090s, with some spots showing higher values near the building surfaces (Case 24). Under SSP5-8.5, with the inflow temperature increasing by 2.9 °C in the 2090s, the AT increase in the entire district was evident (Case 27). When viewed simultaneously with the MRT results, the values tended to be even higher in the sunlit areas.

Focusing on the AT results for the north-south road in **Fig. 11** under any SSP/RCP, the numerical changes were larger in the cases of only temperature rise (red line) than only changes in building stocks (blue line). Under all SSP/RCP, in the cases of only changes in building stocks (Case 1–9), the differences from the base year were within 0.5 °C. In the cases of only temperature rise (Case 10–18), the numerical changes were relatively large and directly linked to the inflow temperatures. For example, the increases from the base year to the 2090s were 0.3 °C, 1.4 °C, and 2.5 °C for SSP1-2.6, SSP2-4.5, and SSP5-8.5, respectively (Case 12, 15, and 18). These values were roughly proportional to the increases in inflow temperature of 0.4 °C, 1.7 °C, and 2.9 °C. Based on these results, the numerical changes in the cases of both changes (Case 19–27, yellow line) tended to be close to those in the cases of only temperature rise (Case 10–18).

Focusing on the AT results for the east-west road in **Fig. 11**, the overall trend was similar to that for the north-south road, and the numerical changes were larger in the cases of only temperature rise (red line) than only changes in building stocks (blue line). There were no significant differences between the values for north-south and east-west roads in the same case. Under all SSP/RCP, in the cases of only changes in building stocks (Case 1–9), the numerical changes from the base year were within 0.6 °C. In the cases of only

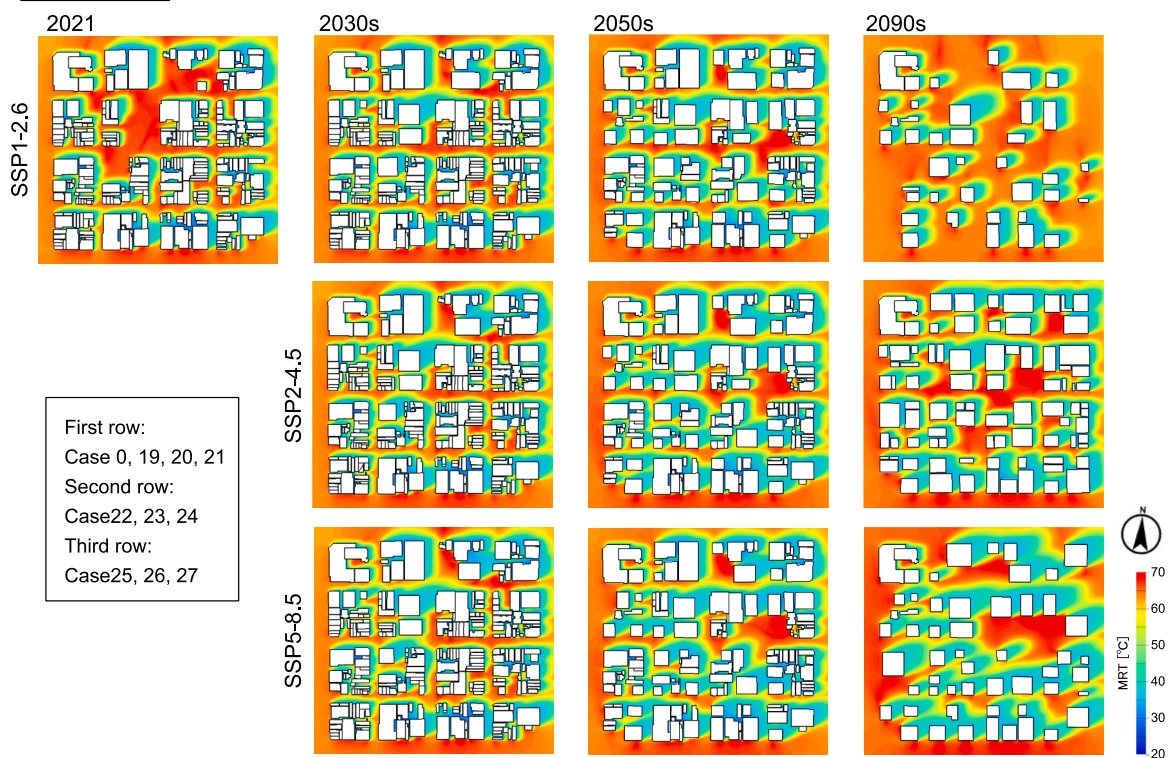
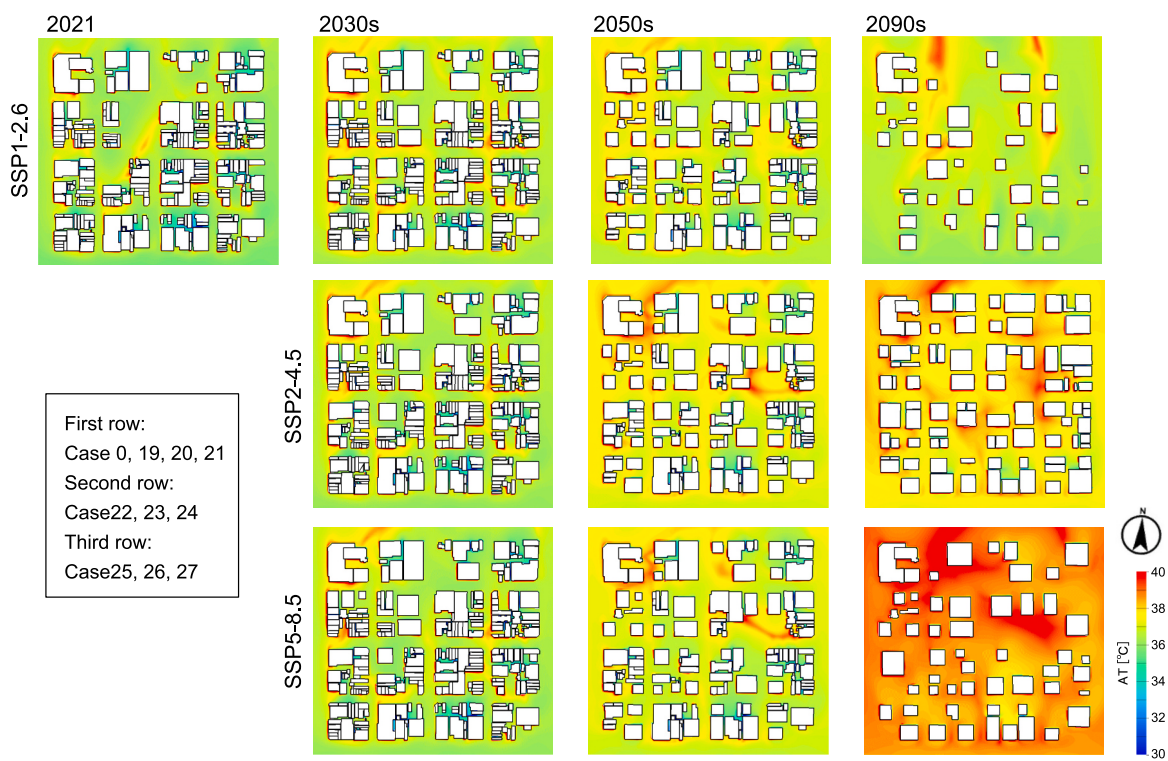
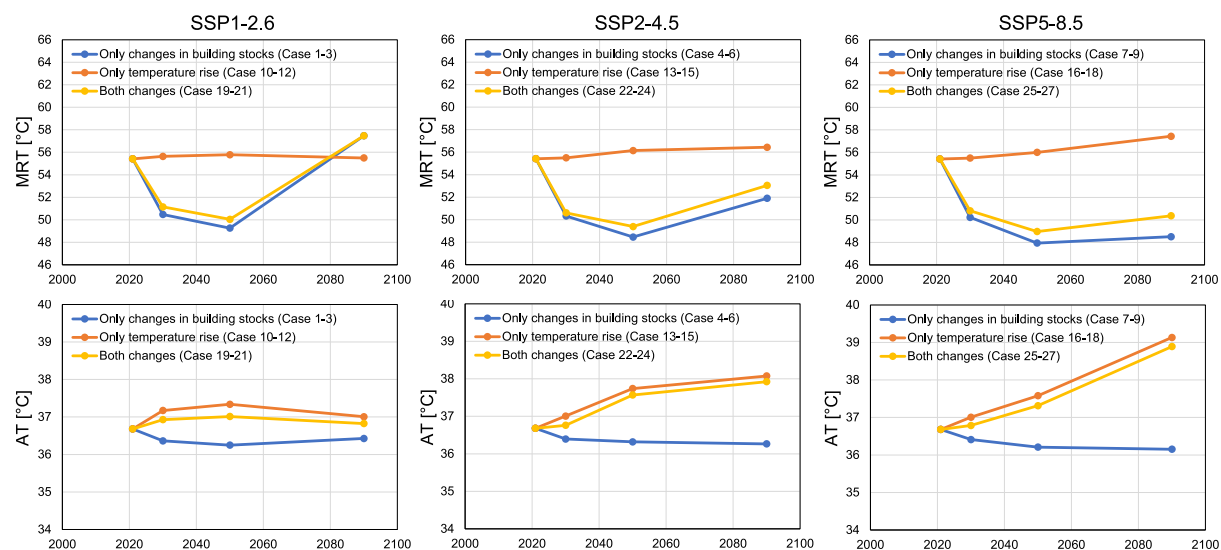
MRT at 14:00AT at 14:00

Fig. 10. Analysis results (Case 0 and Case 19–27): spatial distributions of the MRT and AT at 1.1 m above the ground at 14:00 for each year.

## North-south road at 14:00



## East-west road at 14:00

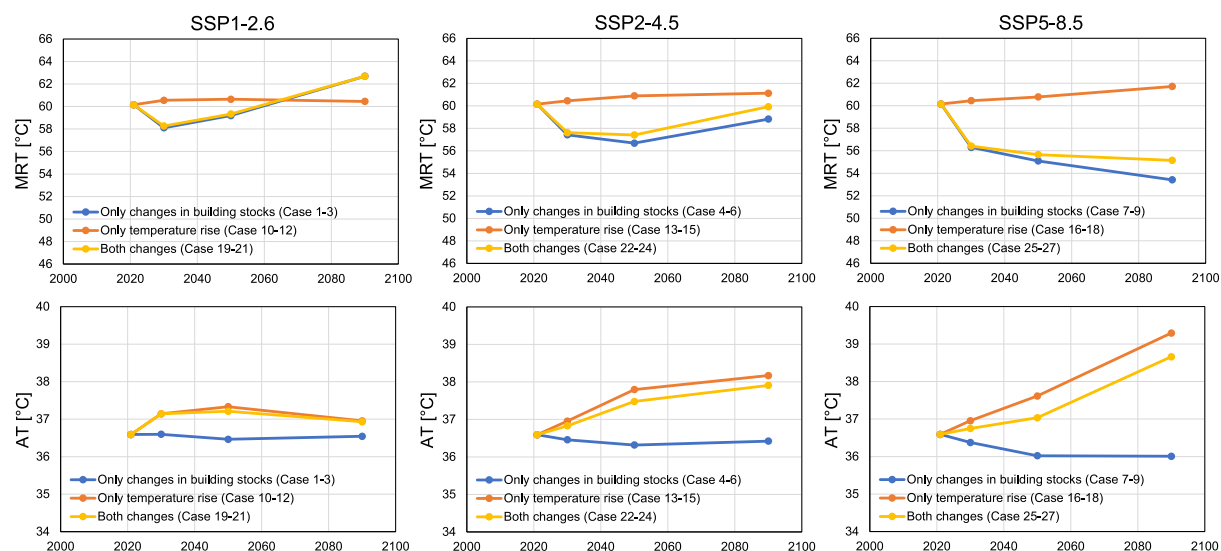


Fig. 11. Analysis results (Case 0–27): Changes in average values of the MRT and AT at 1.1 m above the ground at 14:00 for each year.

Table 7

Differences in average values of the MRT and AT at 1.1 m above the ground between 2021 and the 2090s at 14:00 under each SSP/RCP (Case 0–27).\*

Case		MRT [°C]			AT [°C]		
		SSP 1-2.6	SSP 2-4.5	SSP 5-8.5	SSP 1-2.6	SSP 2-4.5	SSP 5-8.5
North-south Road	Only changes in building stocks	2.0	−3.5	−6.9	−0.3	−0.4	−0.5
	Only temperature rise	0.1	1.0	2.0	0.3	1.4	2.5
	Both changes	2.0	−2.4	−5.1	0.1	1.2	2.2
East-west Road	Only changes in building stocks	2.5	−1.3	−6.7	0.0	−0.2	−0.6
	Only temperature rise	0.3	1.0	1.6	0.4	1.6	2.7
	Both changes	2.5	−0.2	−5.0	0.3	1.3	2.1

\* Negative numbers indicate a decrease in value from 2021 to the 2090s.

temperature rise (Case 10–18), the increases from the base year to the 2090s were 0.4 °C, 1.6 °C, and 2.7 °C for SSP1-2.6, SSP2-4.5, and SSP5-8.5, respectively. These values were also approximately proportional to the increase in the inflow temperature.

### 3.2.2. Results of diurnal changes in the 2090s

Fig. 12 shows the spatial distributions of the MRT and AT at 1.1 m above the ground for the entire district every two hours from 10:00 for Case 21, 24, and 27. Thus, it is possible to compare the diurnal changes when both changes in building stocks and temperature rises are reflected in the 2090s under each SSP/RCP. In addition, we calculated the average MRT and AT at 1.1 m above the north-south and east-west roads as representative spaces within the district, as described in Section 3.2.1. Fig. 13 shows the diurnal changes in these average values from 10:00 to 18:00 in the 2090s for the same SSP/RCP. For example, under SSP1-2.6, diurnal changes were observed for Case 0, 3, and 12. Thus, it is possible to compare the diurnal changes reflecting only changes in building stocks and only temperature rise from 2021 to the 2090s under each SSP/RCP. Table 8 shows the maximum differences in these average values from 10:00 to 18:00 between 2021 and the 2090s under each SSP/RCP, serving as a supplement to Fig. 13.

**3.2.2.1. MRT results.** Focusing on the MRT results in Fig. 12, the values for the entire district were largely affected by the distribution of shade owing to building stocks and the altitude and direction of the sun. In each case, at 10:00 and 14:00, the shade of buildings extended diagonally across the block layout, resulting in a relatively expanded area with lower values on both the north-south and east-west roads. Under SSP1-2.6 (Case 21), there were fewer buildings, resulting in a relatively smaller shaded area at any time. Under SSP2-4.5 (Case 24), despite having the largest number of buildings, the area shaded by buildings was smaller than that under SSP5-8.5 (Case 27), leaving some parts unshaded throughout the day. Under SSP5-8.5 (Case 27), the high-rise buildings created a large, shaded area, resulting in few parts not being shaded throughout the day. Under SSP2-4.5 and SSP5-8.5, the values in the sunlit area tended to be higher than those under SSP1-2.6, mainly because of the differences in the widths of the building sides and their surface temperatures.

Focusing on the MRT results for both roads in Fig. 13 under any SSP/RCP, the differences from the base year (black line) tended to be larger in the cases of only changes in building stocks (blue line) than only temperature rise (red line). In the cases of only changes in building stocks (Case 3, 6, and 9), the differences from the base year were smaller at approximately 12:00 above the north-south road and approximately 16:00 above the east-west road. This is because the effect of building stock was smaller when the sun and roads were aligned in the same direction.

Focusing on the MRT results for the north-south road in Fig. 13, in Case 0, the value reached its maximum (59.2 °C) at 12:40. This was related to factors such as the sun's altitude and direction, shaded areas on the road, and the absorption and reflection of solar radiation by buildings at that time. Under SSP1-2.6, in the case of only temperature rise (Case 12), the maximum difference from Case 0 was 0.6 °C at 10:00. In contrast, in the case of only changes in building stocks (Case 3), the value exceeded that of Case 0 almost throughout the day owing to the decrease in the number of buildings, with the maximum difference being 4.8 °C at 10:00. Under SSP2-4.5 and SSP5-8.5, the differences between the cases of only temperature rise (Case 15 and 18) and Case 0 were relatively small, with the maximum differences from Case 0 being 1.3 °C at 10:00 under SSP2-4.5 and 2.2 °C at 15:30 under SSP5-8.5. In contrast, the values in the cases of only changes in building stocks (Case 6 and 9) were lower than those in Case 0 throughout the day, with the maximum differences from Case 0 being 4.5 °C at 14:10 under SSP2-4.5 and 7.0 °C at 13:40 under SSP5-8.5. Especially under SSP5-8.5, this difference was because the shade from high-rise buildings covered the entire north-south road around 14:00.

Focusing on the MRT results for the east-west road in Fig. 13, in Case 0, the value reached its maximum (60.3 °C) at 14:30. The relationships in the values between the cases under the same SSP/RCP showed a similar trend to those of the north-south road. Under SSP1-2.6, in the case of only temperature rise (Case 12), the maximum difference from Case 0 was 0.8 °C at 17:20. In contrast, in the case of only changes in building stocks (Case 3), there were many times when the value was higher than that in Case 0, with the maximum difference being 3.4 °C at 12:50, indicating the effect of the decrease in the number of buildings. Under SSP2-4.5 and SSP5-8.5, the differences between the cases of only temperature rise (Case 15 and 18) and Case 0 were relatively small, with the maximum differences from Case 0 being 1.3 °C at 12:10 under SSP2-4.5 and 1.9 °C at 18:00 under SSP5-8.5. In contrast, the values in the cases of only changes in building stocks (Case 6 and 9) were lower than those in Case 0 throughout the day, with the maximum differences from Case 0 being 3.5 °C at 17:20 under SSP2-4.5 and 7.1 °C at 10:00 under SSP5-8.5. These maximum differences were similar to those of the north-south road; however, the times they occurred differed.

**3.2.2.2. AT results.** Focusing on the AT results in Fig. 12, the values for the entire district were relatively high at 14:00 in each case and likely depended on the inflow temperature. The values were relatively higher near building surfaces exposed to direct solar radiation, and the parts varied depending on the direction of the sun. Under SSP1-2.6 (Case 21), warmed air did not accumulate significantly because fewer buildings existed. Under SSP2-4.5 (Case 24) and SSP5-8.5 (Case 27), there were relatively many buildings and some spots where the values were higher near the building surfaces. When viewed simultaneously with the MRT results, the values tended to be even higher in the sunlit areas each time. As a result, there were some areas where the AT exceeded 40 °C at 14:00 under SSP5-8.5.

Focusing on the AT results for both roads in Fig. 13 under any SSP/RCP, the differences from the base year (black line) tended to be larger in the cases of only temperature rise (red line) than only changes in building stocks (blue line). In the MRT results, the values often decreased significantly in cases of only changes in building stocks (Case 3, 6 and 9), but these effects were limited in the AT results. In general, similar diurnal changes were observed on both roads. Under SSP1-2.6, there were relatively few differences in Case 3 and 12 compared to Case 0. Under SSP2-4.5 and SSP5-8.5, the values in the cases of only temperature rise (Case 15 and 18) were significantly higher than those in Case 0 throughout the day. Regarding the daily average values for the north-south road, there was a

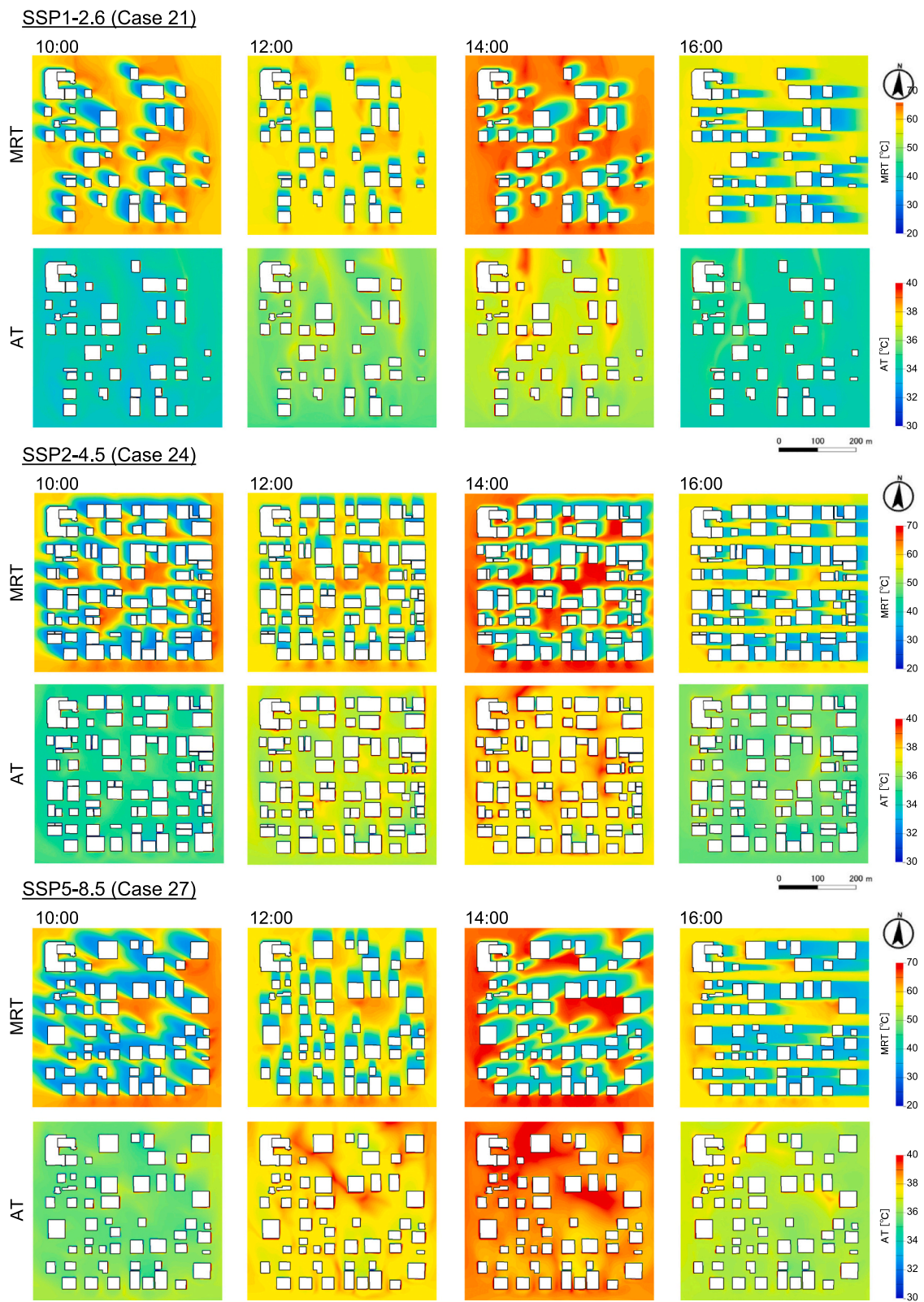
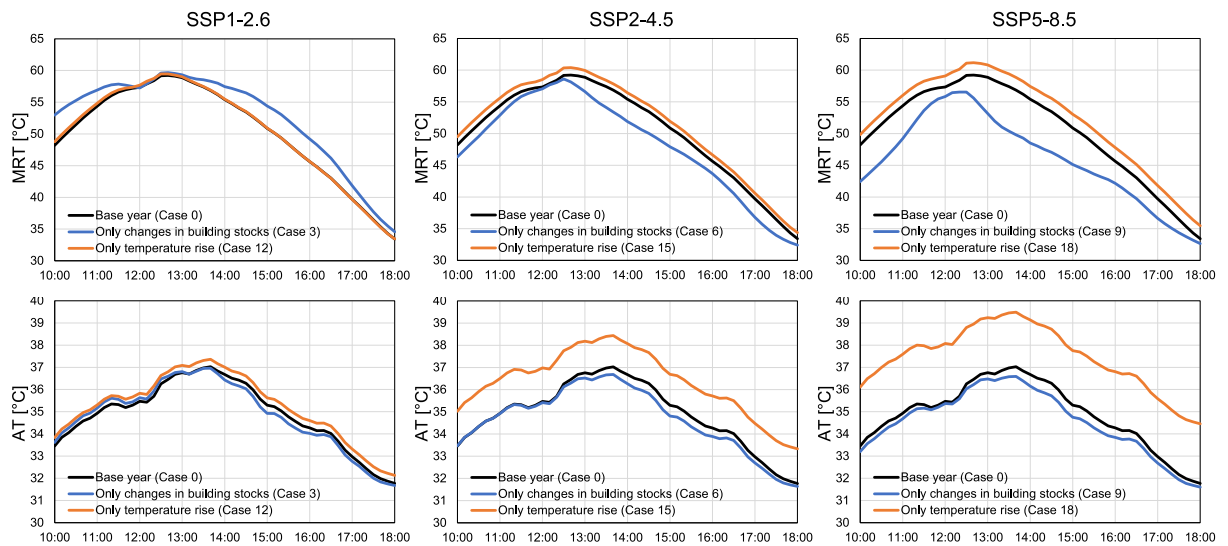


**Fig. 12.** Analysis results (Case 21, 24, and 27): spatial distributions of the MRT and AT at 1.1 m above the ground every two hours from 10:00 in the 2090s.

### North-south road in the 2090s



### East-west road in the 2090s

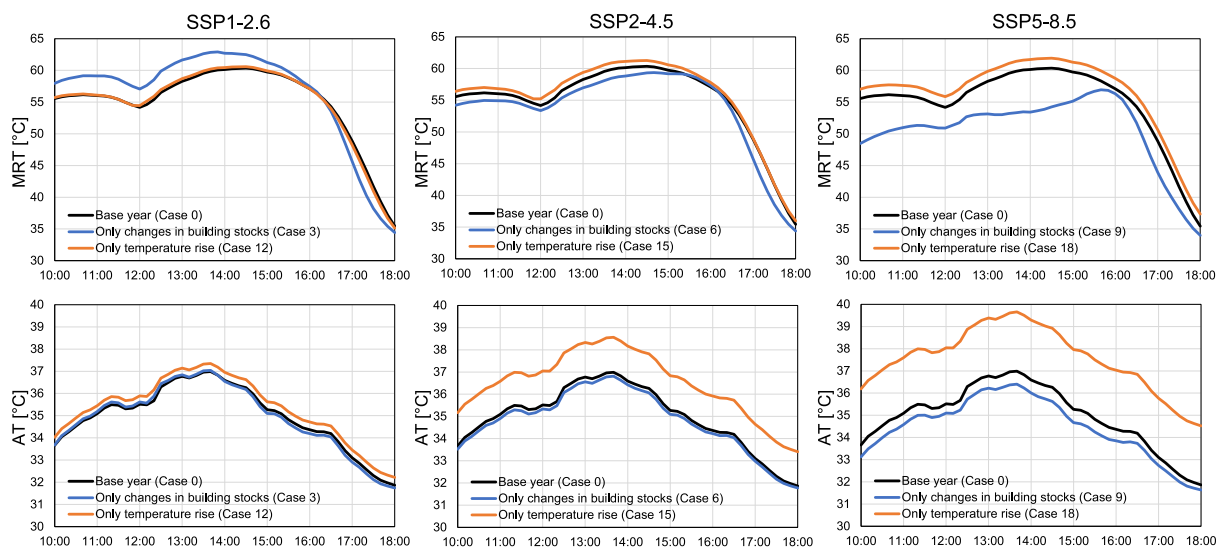


**Fig. 13.** Analysis results (Case 0, 3, 6, 9, 12, 15, and 18): diurnal changes in average values of the MRT and AT at 1.1 m above the ground from 10:00 to 18:00 in the 2090s.

**Table 8**

maximum differences in average values of the MRT and AT at 1.1 m above the ground from 10:00 to 18:00 between 2021 and the 2090s under each SSP/RCP (Case 0, 3, 6, 9, 12, 15, and 18).\*

Case		MRT [°C]			AT [°C]		
		SSP 1-2.6	SSP 2-4.5	SSP 5-8.5	SSP 1-2.6	SSP 2-4.5	SSP 5-8.5
North-south Road	Only changes in building stocks	4.8	-3.5	-7.0	-0.4	-0.5	-0.6
	Only temperature rise	0.6	1.3	2.2	0.5	1.6	2.7
East-west Road	Only changes in building stocks	3.4	-3.5	-7.1	-0.2	-0.2	-0.6
	Only temperature rise	-0.8	1.3	1.9	0.5	1.7	2.7

\* Negative numbers indicate a decrease in value from 2021 to the 2090s.

difference of 0.3 °C in Case 12, 1.5 °C in Case 15, and 2.6 °C in Case 18 compared to Case 0. Similarly for the east-west road, there was a difference of 0.3 °C in Case 12, 1.5 °C in Case 15, and 2.6 °C in Case 18 compared to Case 0. These differences were approximately proportional to the increases in inflow temperature of 0.4 °C, 1.7 °C, and 2.9 °C between SSP/RCP cases.

## 4. Discussion

### 4.1. Interpretation of results

Based on the results in Section 3.2, we were able to understand the relative effects of future changes in building stocks and temperature rises on the microclimate in the district compared with those of the base year. Overall, the results indicated that changes in building stocks tend to mainly affect MRT, and temperature rises tend to mainly affect AT. An overview of the results in Section 3.2.1 (at 14:00 for each year) showed that in the cases of only changes in building stocks, the maximum difference from the base year was −7.5 °C for MRT (north-south road, 2050s, SSP5-8.5) and −0.6 °C for AT (east-west road, 2090s, SSP5-8.5). In the cases of only temperature rise, the maximum difference from the base year was +2.0 °C for MRT (north-south road, 2090s, SSP5-8.5) and +2.7 °C for AT (east-west road, 2090s, SSP5-8.5). An overview of the results in Section 3.2.2 (diurnal changes in the 2090s) showed that in the cases of only changes in building stocks, the maximum difference from the base year was −7.1 °C for MRT (east-west road, 10:00, SSP5-8.5) and −0.6 °C for AT (east-west road, 14:30, SSP5-8.5). In the cases of only temperature rise, the maximum difference from the base year was +2.2 °C for MRT (north-south road, 15:30, SSP5-8.5) and +2.7 °C for AT (north-south road, 12:20, SSP5-8.5). These results suggest that while future temperature rises directly affects the district-scale AT, changes in building stocks have the potential to mitigate the effects of temperature rises on human comfort and heat-related risk. We were able to make this suggestion by projecting both future changes and preparing enough cases to understand the effects of each. To verify this suggestion more accurately, it is necessary to integrate and compare the changes in MRT and AT. In the future, we aim to conduct a comprehensive evaluation of how human comfort and heat-related risk changes in each case, using inclusive indicators such as Standard New Effective Temperature (SET\*), Wet-Bulb Globe Temperature (WBGT), Universal Thermal Climate Index (UTCI).

The results in Section 3.2 suggest that under SSP5-8.5, the increased number of high-rise buildings and increased shaded areas often led to preferable conditions for the thermal environment. Nevertheless, it is important to ensure sufficient sunlight on streets for public life, and the extreme intensification of high-rise buildings may violate the preservation of urban landscapes. In contrast, under SSP1-2.6, the environment often did not demonstrate a better thermal outcome due to decreased shaded areas. However, a district with ample open space can have sufficient room to design a physical environment, such as installing sidewalk roofs and greening the ground. For future urban planning, it is necessary to maximize the benefits of shade and concurrently develop environmentally friendly measures that comprehensively consider the various effects on the thermal environment. Current Japanese laws impose several restrictions on building height and the use of open spaces, and new directions and flexible responses may be required for climate change adaptation.

### 4.2. Comparison with previous studies

The results of future MRT and AT in this study were compared with those of previous studies. Conry et al. (2015) and Tumini et al. (2016), described in Section 1, are examples of studies on future microclimates that explicitly present related projection data. First, Conry et al. (2015) simulated microclimates for a university campus and a residential area in Chicago, USA, on a representative summer day. Their study showed that the MRT in the analysis site increased by 3.0 °C at 12:00 in the 2080s compared to the 2010s based on RCP8.5. Our study showed that the MRT increased by 1.7 °C at 12:00 in the 2090s compared to 2021 in the case of only temperature rise, above the north-south road, under SSP5-8.5. Second, Tumini et al. (2016) simulated microclimates for a plaza and surrounding buildings in Concepción, Chile, on a representative summer day. Their study showed that the average daily AT in the analysis site increased by 1.02 °C, 1.60 °C, and 2.70 °C in 2020, 2050, and 2080, respectively, compared to the base year of 1960–1991 based on the A2 ‘medium-high’ GHG emissions scenario. Our study showed that the average AT from 10:00 to 18:00 increased by 0.4 °C, 1.0 °C, and 2.6 °C in the 2030s, 2050s, and 2090s, respectively, compared to 2021 in the case of only temperature rise, above the north-south road, under SSP5-8.5. Given the differences in the various conditions, including the use of CFD software, we confirmed no uninterpretable differences between the results of previous studies and our study.

### 4.3. Limitations

The analysis conditions of this study have a few issues, and caution is required when interpreting our results.

#### 4.3.1. Projection of change in building stocks

In this study, future changes in building stocks were determined through expert judgment. This approach allowed us to prepare future images that closely reflected the district context, although the accuracy of the projection could not be taken for granted. As mentioned in Section 1, the future changes are largely complex and uncertain, making the projection more difficult, especially in urban center districts with high development pressure. Therefore, in this study, modeling the future changes in building stocks should be conceived as “assuming,” not “projecting,” in the district. Specifically, in Section 2.3.2, we intentionally assumed contrasting future development trends under SSP1 and SSP5. For example, SSP1 was designed to have fewer buildings, whereas SSP5 was designed to have more and higher buildings. Subsequently, their spectrum would likely represent the scope of development trends, where the actual course of the

development process might advance, and provide initial insight toward particular projections. For more accurate projections, there may be inquiries into the developmental intentions of various stakeholders, including property owners and landowners.

#### 4.3.2. Projection of temperature rises

In this study, we referred to a high-resolution climate scenario dataset and determined the inflow temperature by uniformly reflecting future temperature rises. However, our analysis could not reflect the intensity and frequency of extreme weather events. In recent years, studies on downscaling methods for GCM have progressed, and statistical, dynamical, and hybrid methods have been developed (Zou et al., 2023). Iizuka (2018) developed a method to downscale GCM data to the building scale using models based on Weather Research and Forecasting (WRF) and Large-Eddy Simulation (LES). Thus, it may be possible to comprehensively assess the impacts of climate change using these methods. For a more in-depth analysis, it may be necessary to simulate the thermal environment under extreme conditions at the district scale, considering the intensity and frequency of heat events that may occur in Japan.

#### 4.3.3. Technical issues of CFD analysis

As we primarily focused on comparing current and future microclimates in this study, the analysis model was intentionally kept relatively simple. This is because if the analysis conditions were set in detail, projecting their future conditions would be difficult. Due to this constraint, a few technical issues arose in the analysis, as described below.

First, the boundary conditions for the building and ground surfaces were set uniformly, and material differences, such as building surface materials including window glass, and those between sidewalks and roads, were not considered. This issue particularly affected the MRT results. Second, the heat exhaust from buildings and traffic was not considered. As the target district is a commercial and business area, there may be a particularly large amount of building heat exhaust during the daytime. However, most high-rise buildings exhaust heat from their rooftops; thus, the direct effects on living spaces may be limited. Third, the buildings surrounding the district and their future forms were not modeled. These factors affect the wind patterns, shading, and inflow temperatures within the district. Fourth, humidity was not analyzed. This analysis did not model trees or water surfaces that affect humidity within the district; however, these factors are essential for verifying SET\*, WBGT, and UTCI. Fifth, the wind direction and speed were kept constant and diurnal changes were not considered. Wind inflow from directions other than the southern side of the model must be identified.

To maintain the practical feasibility of CFD analysis in urban planning, it is necessary to consider data availability and the duration of the analysis. In the future, we aim to address the technical issues while considering these constraints.

## 5. Conclusions

In this study, we conducted future microclimate simulations that reflects changes in building stocks and temperature rises based on SSP/RCP, focusing on the urban central district in Japan. While the results showed that AT increased by up to 2.7 °C due to inflow temperature rises, MRT decreased by up to 7.5 °C due to changes in building stocks by the 2090s above the road at 14:00 on a representative summer day. Thus, it was suggested that while future temperature rises directly affected the district-scale AT, changes in building stocks had the potential to mitigate their effects on human comfort and heat-related risk. Based on them, this study concludes as follows.

- For future climate change impacts on urban areas, it is important to address district-scale adaptation strategies such as effective building stocks management, as well as mitigation strategies for temperature rise through reductions in greenhouse gas emissions and wide-scale heat island measures.
- For future microclimate simulation studies, it is important to prepare scenarios for not only weather conditions but also urban forms based on the development trends within the same framework, and to set cases in order to understand the effects of each change.

By utilizing the knowledge of both climate and urban sciences in case setting, this study created new examples of collaboration between the two disciplines. We expect that our findings will contribute to the creation of scientific evidence to promote climate change adaptation in cities worldwide.

#### CRedit authorship contribution statement

**Junya Yamasaki:** Writing – review & editing, Writing – original draft, Visualization, Validation, Software, Resources, Project administration, Methodology, Investigation, Formal analysis, Conceptualization. **Yasutaka Wakazuki:** Writing – review & editing, Resources, Methodology. **Satoru Iizuka:** Writing – review & editing, Supervision, Methodology. **Takahiro Yoshida:** Writing – review & editing, Conceptualization. **Ryoichi Nitani:** Writing – review & editing, Methodology, Investigation, Conceptualization. **Rikutarō Manabe:** Writing – review & editing, Methodology, Investigation, Funding acquisition, Conceptualization. **Akito Murayama:** Writing – review & editing, Supervision, Project administration, Methodology, Investigation, Funding acquisition, Conceptualization.

#### Declaration of generative AI and AI-assisted technologies in the writing process

Statement: During the preparation of this study, the authors used ChatGPT 3.5, provided by OpenAI, to assist in writing the original draft. After using this service, the authors reviewed and edited the content as needed and take full responsibility for the content of the publication.

## Declaration of competing interest

The authors declare that they have no known competing financial interests or personal relationships that could have appeared to influence the work reported in this paper.

## Data availability

Data will be made available on request.

## Acknowledgements

This study was performed by the Environment Research and Technology Development Fund (JPMEERF20S11817) of the Environmental Restoration and Conservation Agency provided by the Ministry of the Environment of Japan. The authors express their gratitude to Shinya Kuroiwa and Daisuke Kantani, Advanced Knowledge Laboratory, Inc., Yasushi Ishimaru, Ryosuke Arashi (at that time), and Yusuke Kamiya, Center for Environmental Information Science, Ryohei Fukuyama (at that time), The University of Tokyo, for their valuable cooperation while conducting this study. The authors would like to thank Editage ([www.editage.jp](http://www.editage.jp)) for English language editing.

## References

- Antoniou, N., Montazeri, H., Neophytou, M., Blocken, B., 2019. CFD simulation of urban microclimate: validation using high-resolution field measurements. *Sci. Total Environ.* 695, 133743. <https://doi.org/10.1016/j.scitotenv.2019.133743>.
- A-PLAT (Climate Change Adaptation Information Platform), 2021. Population estimates for each municipality according to socioeconomic scenarios (Environment Research and Technology Development Fund 2–1805) (in Japanese). <https://adaptation-platform.nies.go.jp/socioeconomic/population.html>. (Accessed 8 Jan 2024).
- A-PLAT (Climate Change Adaptation Information Platform), 2024. List of local climate change adaptation plans. <https://adaptation-platform.nies.go.jp/en/local/plan/list.html> (Accessed 16 May 2024).
- Area Management Network, 2024. What is Area Management? (in Japanese). <https://areamanagementnetwork.jp> (Accessed 16 May 2024).
- Blocken, B., 2015. Computational fluid dynamics for urban physics: importance, scales, possibilities, limitations and ten tips and tricks towards accurate and reliable simulations. *Build. Environ.* 91, 219–245. <https://doi.org/10.1016/j.buildenv.2015.02.015>.
- Bosselmann, P., 2008. *Urban Transformation: Understanding City Design and Form*. Island Press.
- BREEAM, 2024. BREEAM Communities. <https://breeam.com/standards/communities> (Accessed 16 May 2024).
- Caldarice, O., Tollin, N., Pizzorni, M., 2021. The relevance of science-policy-practice dialogue. Exploring the urban climate resilience governance in Italy. *City Territ. Archit.* 8 <https://doi.org/10.1186/s40410-021-00137-y>.
- Chen, H., Matsuhashi, K., Takahashi, K., Fujimori, S., Honjo, K., Gomi, K., 2020a. Adapting global shared socio-economic pathways for national scenarios in Japan. *Sustain. Sci.* 15, 985–1000. <https://doi.org/10.1007/s11625-019-00780-y>.
- Chen, M., Vernon, C.R., Graham, N.T., Hejazi, M., Huang, M., Cheng, Y., Calvin, K., 2020b. Global land use for 2015–2100 at 0.05° resolution under diverse socioeconomic and climate scenarios. *Sci. Data.* 7, 320. <https://doi.org/10.1038/s41597-020-00669-x>.
- Conry, P., Sharma, A., Potosnak, M.J., Leo, L.S., Bensman, E., Hellmann, J.J., Fernando, H.J.S., 2015. Chicago's heat island and climate change: bridging the scales via dynamical downscaling. *J. Appl. Meteorol. Climatol.* 54, 1430–1448. <https://doi.org/10.1175/JAMC-D-14-0241.1>.
- Doblas-Reyes, F.J., Sörensson, A.A., Almazroui, M., Dosio, A., Gutowski, W.J., Haarsma, R., Hamdi, R., Hewitson, B., Kwon, W.-T., Lamptey, B.L., Maraun, D., Stephenson, T.S., Takayabu, I., Terray, L., Turner, A., Zuo, Z., 2021. The physical science basis. Contribution of working group I to the sixth assessment report of the intergovernmental panel on climate change [Masson-Delmotte, V., P. Zhai, A. Pirani, S.L. Connors, C. Péan, S. Berger, N. Caud, Y. Chen, L. Goldfarb, M.I. Gomis, M. Huang, K. Leitzell, E. Lonnoy, J.B.R. Matthews, T.K. Maycock, T. Waterfield, O. Yelekçi, R. Yu, and B. Zhou (eds.)]. Linking global to regional climate change, in: *climate change*. Cambridge university press, Cambridge, United Kingdom and New York, pp. 1363–1512. <https://doi.org/10.1017/9781009157896.012>.
- Dütemeyer, D., Barlag, A.-B., Kuttler, W., Axt-Kittner, U., 2013. Measures against heat stress in the city of Gelsenkirchen. Germany. *ERDE J. Geogr. Soc. Berl.* 144, 181–201. <https://doi.org/10.12854/erde-144-14>.
- Elmqvist, T., Andersson, E., Frantzeskaki, N., McPhearson, T., Olsson, P., Gaffney, O., Takeuchi, K., Folke, C., 2019. Sustainability and resilience for transformation in the urban century. *Nat. Sustain.* 2, 267–273. <https://doi.org/10.1038/s41893-019-0250-1>.
- Emmanuel, R., Loconsole, A., 2015. Green infrastructure as an adaptation approach to tackling urban overheating in the Glasgow Clyde valley region. *UK. Landsc. Urban Plan.* 138, 71–86. <https://doi.org/10.1016/j.landurbplan.2015.02.012>.
- Fahmy, M., Mahdy, M., Mahmoud, S., Abdelalim, M., Ezzeldin, S., Attia, S., 2020. Influence of urban canopy green coverage and future climate change scenarios on energy consumption of new sub-urban residential developments using coupled simulation techniques: a case study in Alexandria. *Egypt. Energy Rep.* 6, 638–645. <https://doi.org/10.1016/j.egy.2019.09.042>.
- Gao, J., O'Neill, B.C., 2020. Mapping global urban land for the 21st century with data-driven simulations and shared socioeconomic pathways. *Nat. Commun.* 11, 2302. <https://doi.org/10.1038/s41467-020-15788-7>.
- Greger, K., 2015. Spatio-temporal building population estimation for highly urbanized areas using GIS. *Trans. GIS* 19, 129–150. <https://doi.org/10.1111/tgis.12086>.
- Grossman-Clarke, S., Schubert, S., Fenner, D., 2017. Urban effects on summertime air temperature in Germany under climate change. *Int. J. Climatol.* 37, 905–917. <https://doi.org/10.1002/joc.4748>.
- Heywood, P., 2023. *Planning for Community*. Wiley.
- Iizuka, S., 2018. Future environmental assessment and urban planning by downscaling simulations. *J. Wind Eng. Ind. Aerodyn.* 181, 69–78. <https://doi.org/10.1016/j.jweia.2018.08.015>.
- International Living Future Institute, 2024. Living Community Challenge. <https://living-future.org/lcc> (Accessed 16 May 2024).
- IPCC, 2021. *The Physical Science Basis. Contribution of Working Group I to the Sixth Assessment Report of the Intergovernmental Panel on Climate Change* [Masson-Delmotte, V., P. Zhai, A. Pirani, S.L. Connors, C. Péan, S. Berger, N. Caud, Y. Chen, L. Goldfarb, M.I. Gomis, M. Huang, K. Leitzell, E. Lonnoy, J.B.R. Matthews, T.K. Maycock, T. Waterfield, O. Yelekçi, R. Yu, and B. Zhou (eds.)]. Summary for policymakers, in: *Climate Change*. Cambridge University Press, Cambridge, United Kingdom and New York.
- IPCC, 2022. *Impacts, Adaptation, and Vulnerability. Contribution of Working Group II to the Sixth Assessment Report of the Intergovernmental Panel on Climate Change* [H.-O. Pörtner, D.C. Roberts, M. Tignor, E.S. Poloczanska, K. Mintenbeck, A. Alegría, M. Craig, S. Langsdorf, S. Löschke, V. Möller, A. Okem, B. Rama (eds.)]. Summary for policymakers, in: Pörtner, H.-O., Roberts, D.C., Poloczanska, E.S., Mintenbeck, K., Tignor, M., Alegría, A., Craig, M., Langsdorf, S., Löschke, S., Möller, V., Okem, A. (Eds.). *Climate Change*. Cambridge University Press, Cambridge, United Kingdom and New York.

- Ishizaki, N.N., Shioyama, H., Hanasaki, N., Takahashi, K., 2022. Development of CMIP6-based climate scenarios for Japan using statistical method and their applicability to heat-related impact studies. *Earth Space Sci.* 9, 1–12. <https://doi.org/10.1029/2022EA002451>.
- ISO, 1998. *ISO7726: Ergonomics of the Thermal Environment—Instruments for Measuring Physical Quantities*.
- Just Communities, 2024. Just Communities | The Evolution of Ecodistricts. <https://justcommunities.info> (Accessed 16 May 2024).
- Kaoru, I., Akira, K., Akikazu, K., 2011. The 24-h unsteady analysis of air flow and temperature in a real city by high-speed radiation calculation method. *Build. Environ.* 46, 1632–1638. <https://doi.org/10.1016/j.buildenv.2011.01.029>.
- Kaplan, S., Georgescu, M., Alfasi, N., Kloog, I., 2017. Impact of future urbanization on a hot summer: a case study of Israel. *Theor. Appl. Climatol.* 128, 325–341. <https://doi.org/10.1007/s00704-015-1708-3>.
- Kimura, F., Kitoh, A., 2007. Downscaling by pseudo global warming method. The final report of ICCAP. Research Institute for Humanity and Nature (RIHN) 43–46.
- Li, X., Mitra, C., Dong, L., Yang, Q., 2018. Understanding land use change impacts on microclimate using weather research and forecasting (WRF) model. *Phys. Chem. Earth Parts A B C.* 103, 115–126. <https://doi.org/10.1016/j.pce.2017.01.017>.
- Li, M., Zhou, B.B., Gao, M., Chen, Y., Hao, M., Hu, G., Li, X., 2022. Spatiotemporal dynamics of global population and heat exposure (2020–2100): based on improved SSP-consistent population projections. *Environ. Res. Lett.* 17, 094007 <https://doi.org/10.1088/1748-9326/ac8755>.
- Luederitz, C., Lang, D.J., Von Wehrden, H., 2013. A systematic review of guiding principles for sustainable urban neighborhood development. *Landsc. Urban Plan.* 118, 40–52. <https://doi.org/10.1016/j.landurbplan.2013.06.002>.
- Lwin, K., Murayama, Y., 2009. A GIS approach to estimation of building population for micro-spatial analysis. *Trans. GIS* 13, 401–414. <https://doi.org/10.1111/j.1467-9671.2009.01171.x>.
- McNamara, K.E., Buggy, L., 2017. Community-based climate change adaptation: a review of academic literature. *Local Environ.* 22, 443–460. <https://doi.org/10.1080/13549839.2016.1216954>.
- Middel, A., Chhetri, N., Quay, R., 2015. Urban forestry and cool roofs: assessment of heat mitigation strategies in Phoenix residential neighborhoods. *Urban For. Urban Green.* 14, 178–186. <https://doi.org/10.1016/j.ufug.2014.09.010>.
- Mirzaei, P.A., 2021. CFD modeling of micro and urban climates: problems to be solved in the new decade. *Sustain. Cities Soc.* 69, 102839 <https://doi.org/10.1016/j.scs.2021.102839>.
- MOE (Ministry of the Environment. Japan), 2020. Climate change impact assessment report (in Japanese). <https://www.env.go.jp/content/900516663.pdf> (Accessed 8 Jan 2024).
- MOE (Ministry of the Environment. Japan), 2021. Climate change adaptation plan (in Japanese). <https://www.env.go.jp/content/000138042.pdf> (Accessed 8 Jan 2024).
- Montazeri, H., Toparlal, Y., Blocken, B., Hensen, J.L.M., 2017. Simulating the cooling effects of water spray systems in urban landscapes: a computational fluid dynamics study in Rotterdam. The Netherlands. *Landsc. Urban Plan.* 159, 85–100. <https://doi.org/10.1016/j.landurbplan.2016.10.001>.
- Murakami, D., Yoshida, T., Yamagata, Y., 2021. Gridded GDP projections compatible with the five SSPs (shared socioeconomic pathways). *Front. Built Environ.* 7, 760306 <https://doi.org/10.3389/fbuil.2021.760306>.
- Nagoya City, 2020. Nagoya City Urban Planning Master Plan 2030 (in Japanese). <https://www.city.nagoya.jp/jutakutoshi/cmsfiles/contents/0000002/2733/gaiyouban.pdf>. (Accessed 16 May 2024).
- Nishiki 2 Area Management, 2024. NISHIKI2 (in Japanese). <http://nishiki2areamanagement.co.jp> (Accessed 16 May 2024).
- Nishiki 2 District Community Development Council, 2011. Nishiki 2 District Choja-machi Master Plan (2011–2030) (in Japanese).
- Olén, N.B., Lehsten, V., 2022. High-resolution global population projections dataset developed with CMIP6 RCP and SSP scenarios for year 2010–2100. *Data Brief* 40, 107804. <https://doi.org/10.1016/j.dib.2022.107804>.
- O'Neill, B.C., Krieger, E., Riahi, K., Ebi, K.L., Hallegatte, S., Carter, T.R., Mathur, R., van Vuuren, D.P., 2014. A new scenario framework for climate change research: the concept of shared socioeconomic pathways. *Clim. Chang.* 122, 387–400. <https://doi.org/10.1007/s10584-013-0905-2>.
- Owen, G., 2020. What makes climate change adaptation effective? A systematic review of the literature. *Glob. Environ. Chang.* 62, 102071 <https://doi.org/10.1016/j.gloenvcha.2020.102071>.
- Peng, C., Elwan, A., 2014. An outdoor-indoor coupled simulation framework for climate change-conscious urban neighborhood design. *Simulation* 90, 874–891. <https://doi.org/10.1177/0037549714526293>.
- Piggott-McKellar, A.E., McNamara, K.E., Nunn, P.D., Watson, J.E.M., 2019. What are the barriers to successful community-based climate change adaptation? A review of grey literature. *Local Environ.* 24, 374–390. <https://doi.org/10.1080/13549839.2019.1580688>.
- Qiu, Y., Zhao, X., Fan, D., Li, S., Zhao, Y., 2022. Disaggregating population data for assessing progress of SDGs: methods and applications. *Int. J. Digit. Earth.* 15, 2–29. <https://doi.org/10.1080/107538947.2021.2013553>.
- Sadeghi, M., Karimi, M., Rabiei-Dastjerdi, H., Sarkar, D., 2023. Adaptive weighted least squares (AWLS): a new vector-based model to improve urban population estimation at small-area scale using morphology and attractiveness criteria. *Appl. Geogr.* 158, 103050 <https://doi.org/10.1016/j.apgeog.2023.103050>.
- Shi, L., Chu, E., Anguelovski, I., Aylett, A., Debats, J., Goh, K., Schenk, T., Seto, K.C., Dodman, D., Roberts, D., Roberts, J.T., Vandever, S.D., 2016. Roadmap towards justice in urban climate adaptation research. *Nat. Clim. Chang.* 6, 131–137. <https://doi.org/10.1038/nclimate2841>.
- Tominaga, Y., Wang, L.L., Zhai, Z.J., Stathopoulos, T., 2023. Accuracy of CFD simulations in urban aerodynamics and microclimate: Progress and challenges. *Build. Environ.* 243, 110723 <https://doi.org/10.1016/j.buildenv.2023.110723>.
- Toparlal, Y., Blocken, B., Vos, P., van Heijst, G.J.F., Janssen, W.D., van Hooff, T., Montazeri, H., Timmermans, H.J.P., 2015. CFD simulation and validation of urban microclimate: a case study for Bergpolder Zuid. Rotterdam. *Build. Environ.* 83, 79–90. <https://doi.org/10.1016/j.buildenv.2014.08.004>.
- Toparlal, Y., Blocken, B., Maiheu, B., van Heijst, G.J.F., 2017. A review on the CFD analysis of urban microclimate. *Renew. Sust. Energ. Rev.* 80, 1613–1640. <https://doi.org/10.1016/j.rser.2017.05.248>.
- Tsoka, S., Velikou, K., Tolika, K., Tsikaloudaki, A., 2021. Evaluating the combined effect of climate change and urban microclimate on buildings' heating and cooling energy demand in a Mediterranean city. *Energies* 14, 5799. <https://doi.org/10.3390/en14185799>.
- Tumini, I., Rubio-Bellido, C., 2016. Measuring climate change impact on urban microclimate: a case study of Concepción. *Procedia Eng.* 161, 2290–2296. <https://doi.org/10.1016/j.proeng.2016.08.830>.
- U.S. Green Building Council, 2024. LEED for Cities and Communities. <https://www.usgbc.org/leed/rating-systems/leed-for-cities-communities> (Accessed 16 May 2024).
- van Vuuren, D.P., Edmonds, J., Kainuma, M., Riahi, K., Thomson, A., Hibbard, K., Hurtt, G.C., Kram, T., Krey, V., Lamarque, J.-F., Masui, T., Meinshausen, M., Nakicenovic, N., Smith, S.J., Rose, S.K., 2011. The representative concentration pathways: an overview. *Clim. Chang.* 109, 5–31. <https://doi.org/10.1007/s10584-011-0148-z>.
- von Wirth, T., Wissen Hayek, U.W., Kunze, A., Neuenschwander, N., Stauffacher, M., Scholz, R.W., 2014. Identifying urban transformation dynamics: functional use of scenario techniques to integrate knowledge from science and practice. *Technol. Forecasting Soc. Change.* 89, 115–130. <https://doi.org/10.1016/j.techfore.2013.08.030>.
- Wai, K.-M., Xiao, L., Tan, T.Z., 2021. Improvement of the outdoor thermal comfort by water spraying in a high-density urban environment under the influence of a future (2050) climate. *Sustainability* 13, 7811. <https://doi.org/10.3390/su13147811>.
- Wang, T., Sun, F., 2022. Global gridded GDP data set consistent with the shared socioeconomic pathways. *Sci. Data.* 9, 221. <https://doi.org/10.1038/s41597-022-01300-x>.
- Wang, X., Meng, X., Long, Y., 2022. Projecting 1 km-grid population distributions from 2020 to 2100 globally under shared socioeconomic pathways. *Sci. Data.* 9, 563. <https://doi.org/10.1038/s41597-022-01675-x>.
- Yasui, M., Izumiya, R., 2021. Gakugei shuppansha. Area management case method. Textbook of regional management through public-private collaboration (in Japanese).

- Ye, B., Jiang, J., Liu, J., Zheng, Y., Zhou, N., 2021. Research on quantitative assessment of climate change risk at an urban scale: review of recent progress and outlook of future direction. *Renew. Sust. Energ. Rev.* 135, 110415 <https://doi.org/10.1016/j.rser.2020.110415>.
- Yi, C.Y., Peng, C., 2014. Microclimate change outdoor and indoor coupled simulation for passive building adaptation design. *Procedia Comput. Sci.* 32, 691–698. <https://doi.org/10.1016/j.procs.2014.05.478>.
- Zou, J., Lu, H., Shu, C., Ji, L., Gaur, A., Wang, L., 2023. Multiscale numerical assessment of urban overheating under climate projections: a review. *Urban Clim.* 49, 101551 <https://doi.org/10.1016/j.uclim.2023.101551>.